Sunrise Wind Farm Project

Appendix BB
Intake Zone of Influence and Thermal Discharge Modeling Report

Prepared for:

Sunrise Wind | Powered by Ørsted & Eversource

April 8, 2022

Sunrise Wind Farm Converter Station
Intake Zone of Influence & Thermal Discharge Modeling Report

December 2021

Prepared by:
Woods Hole Group
A CLS Company
107 Waterhouse Road
Bourne, MA

Table of Contents

List of Figures

List of Tables

Symbols and Abbreviations

AC	Alternating Current
COP	Construction and Operations Plan
CORMIX	CORnell MIXing Zone Expert System
CWIS	Cold Water Intake System
DC	Direct Current
FV-COM	Finite-Volume Coastal Ocean Model
IAC	Inter-Array Cables
HZI	Hydraulic Zone of Influence
kV	kilovolt
LMSL	Local Mean Sea Level
LIS	Long Island Sound
MGD	million gallons per day
NECOFS	Northeast Coastal Ocean Forecast System
NPDES	National Pollutant Discharge Elimination System
NFR	Near Field Region
OCS	Outer Continental Shelf
OCS-DC	Offshore Converter Station – Direct Current
OnCS-DC	Onshore Converter Station
SRWF	Sunrise Wind Farm
SRWEC	Sunrise Wind Export Cable
SWLP	Seawater Lift Pump
WTG	Wind Turbine Generator
ΔT	Temperature Differential

1.0 INTRODUCTION

Sunrise Wind, a 50/50 joint venture between Orsted North America Inc. (Orsted NA or Orsted) and Eversource Investment LLC (Eversource), proposes to construct, own, and operate the Sunrise Wind Farm (SRWF) and the Sunrise Wind Export Cable (SRWEC) (collectively, the Sunrise Wind Farm Project or Project). The SRWF will be located on the Outer Continental Shelf (OCS) and includes up to 94 Wind Turbine Generators (WTGs) at 102 potential locations, up to 180 mi (290 km) of Inter-Array Cables (IAC), and an Offshore Converter Station (OCS-DC). The network of alternating current (AC) IAC will carry the electrical current produced by the WTGs to the OCS-DC. The OCS-DC will convert the medium voltage AC generated by the WTGs to direct current (DC) and transfer it to a higher voltage for transmission to the Project's onshore electrical infrastructure (via the SRWEC). An Onshore Converter Station (OnCS-DC) would convert the DC back to AC for interconnection to the electrical grid.

The information and analysis presented in this report was developed in support of a new individual National Pollutant Discharge Elimination System (NPDES) permit under Section 402 of the Clean Water Act. A NPDES individual permit application for the operation of the OCS-DC) located in the Lease Area was submitted to the United States Environmental Protection Agency on December 1, 2021.

The OCS-DC will house both AC and DC equipment up to ±320 kilovolt (kV). The AC to DC conversion process generates heat and, as such, necessitates the use of cooling water to remove excess heat. Cooling water for this process will be extracted through three vertical intake pipes attached to the steel foundation legs of the OCS-DC with openings located at a height 30 ft (10 m) above the seafloor. Water through each of the three vertical intake pipes is withdrawn using a total of three seawater lift pumps (SWLP), a single SWLP dedicated to each intake pipe. Cooling water will pass through a series of heat exchange equipment located on the topside OCS-DC platform and be discharged back to the source water, albeit at a higher temperature, via a single outlet Dump Caisson at a depth of 40 ft (12 m) below Local Mean Sea Level (LMSL).

Cooling water withdrawn through the intake pipes from the OCS source water locally influences currents, both vertically (the w component of velocity), and radially (the u and v components of the velocity). At the Dump Caisson, the thermal effluent outflows also influence the existing source water conditions. The potential influence of this facility while operational as it pertains to water intake and discharge was examined using available data and computer simulations. This memorandum documents the data sources, model theory and application for both the intake and discharge, and preliminary findings to define the intake hydraulic zone of influence (HZI) and the zone of thermal effluent.

2.0 AMBIENT CONDITIONS & PROPOSED CONFIGURATION

The OCS-DC station will be located in ocean waters approximately 148 ft (45 m) deep relative to LMSL with a mean tide range of 3.05 ft (0.93 m). Local currents in the vicinity of the converter station are driven by a combination of winds, tides, and density gradients due to salinity and temperature differences. Velocities in the water column are stratified, with higher velocities near the surface with a time averaged speed of 0.72 ft/s (0.22 m/s) and a time averaged bottom current of 0.25 ft/s (0.08 m/s) during the 1997/1998 year of study consistent with the findings documented in the SRW Construction and Operations Plan (COP) developed for the Project (Orsted, 2021). Temperatures in study area exhibit seasonal variability with higher temperatures in the late summer and early fall leading to stratification vertically within the water column during the warmer months with surface temperatures near 68°F (20°C) and bottom temperatures near 50°F (10°C). During the colder winter months, the thermal stratification is less evident with surface temperatures ranging between 39°F and 41°F (4°C and 5°C), while bottom waters are closer to 41°F (5°C).

The proposed OCS-DC s will withdraw water from the lower sections of the water column through three intake pipes that may be operated individually (i.e., all flow through one intake) or in combination for a total maximum daily flow rate of 8.1 million gallons per day (MGD) (0.35 m^3/s). After passing through the system, the heated water will be discharged via a single caisson with an opening of 5.4 ft^2 (0.5 m^2) at a depth of 40 ft (12 m) below LMSL. Intake and outfall design specifications are listed in Table 2-1 with seasonal flows and temperatures for the heated effluent listed in Table 2-2.

Table 2-1. Intake and outfall design specifications for the OCS-DC.

Cooling Water Intake System Design	
Number of Intakes	3
Height from Seafloor	30 ft (10 m)
Intake Orientation	Downward
Intake Mesh Material	steel
Mesh Size Opening	3 crash bars with dimensions of 2.4 x 0.8 in (60 x 20 mm)
Mesh Configuration	square
Total Intake Opening (per intake)	21.6 ft^2 (2.01 m^2)
Through Screen Intake Velocity (per Intake)	0.43 ft/s (0.13 m/s)
Cooling Water Discharge Design	
Number of Discharges	1
Depth Below LMSL	40 ft (12 m)
Discharge Orientation	Downward
Total Discharge Opening	5.4 ft^2 (0.5 m^2)

Table 2-2. Thermal Discharge Flow Rates and Temperatures for the OCS-DC.

Effluent Flow and Temperature	***JAN***	***FEB***	***MAR***	***APR***	***MAY***	***JUN***	***JUL***	***AUG***	***SEP***	***OCT***	***NOV***	***DEC***
Maximum Average Flow	8.1 MGD	8.1 MGD	8.1 MGD	8.1 MGD	8.1 MGD	8.1 MGD	8.1 MGD	8.1 MGD	8.1 MGD	8.1 MGD	8.1 MGD	8.1 MGD
Daily Average Flow	3.96 MGD	3.96 MGD	3.96 MGD	3.96 MGD	3.96 MGD	3.96 MGD	3.96 MGD	4.31 MGD	4.58 MGD	5.26 MGD	4.89 MGD	4.07 MGD
Maximum Average Temperature	90°F	90°F	90°F	90°F	90°F	90°F	90°F	90°F	90°F	90°F	90°F	90°F
Daily Average Temperature	86°F	86°F	86°F	86°F	86°F	86°F	86°F	86°F	86°F	86°F	86°F	86°F
Monthly Maximum Temperature	90°F	90°F	90°F	90°F	90°F	90°F	90°F	90°F	90°F	90°F	90°F	90°F

3.0 DATA COLLECTION & REVIEW

Ocean currents and temperatures in the vicinity of the proposed OCS-DC were extracted from the Northeast Coastal Ocean Forecast System (NECOFS), which uses the Finite-Volume Coastal Ocean Model (FV-COM) to predict ocean climatology from south of Long Island Sound (LIS) to the north of the Nova Scotian Shelf (UMass Dartmouth MEDM Lab, 2021). The NECOFS model provides hourly hindcast data for ocean currents, water and air temperature, local sea levels, and wave climatology. The efficacy of the NECOFS model was previously verified by Woods Hole Group as part of other assessments for the Project, specifically sediment transport modeling, which identified a year exhibiting climatology that could be classified as an "average" year from the available time series (Woods Hole Group, 2021). For this study, as with the previous sediment transport modeling conducted by Woods Hole Group, model output from September 17, 1997 through September 16, 1998 were used to represent the average annual year of ocean climatology.

At the proposed OCS-DC location, the NECOFS model consists of 45 vertical layers, each approximately 3 ft (1 m) thick, with hourly horizontal velocities (u and v components) and temperatures throughout the water column. The u and v components of the velocity were converted from directional vectors into a current magnitude at each layer using Equation 1.

$$\text{speed} = \sqrt{\text{u}^2 + \text{v}^2} \quad Equation\ 1$$

The time series of ocean current speed in Equation 1 were then plotted as contours as shown on Figure 3-1 . As depicted, the horizontal axis is the time of observation, and the vertical axis is the height above the ocean floor. Apart from several storm events during the winter and spring of 1998, the ocean currents throughout the column tend to be 0.98 ft/s (0.3 m/s) or less throughout the water column, with lower magnitudes near the bottom and higher values near the surface. The largest current observed, with a value of 3.1 ft/s (1.01 m/s) at the surface, occurred on January 17, 1998; however, time-averaged currents in the water column were calculated over the year to be 0.72 ft/s (0.22 m/s) at the surface, and 0.23 ft/s (0.07 m/s) in the bottom layer of the water column, defined as the first 3 ft (1 m) above the ocean floor.

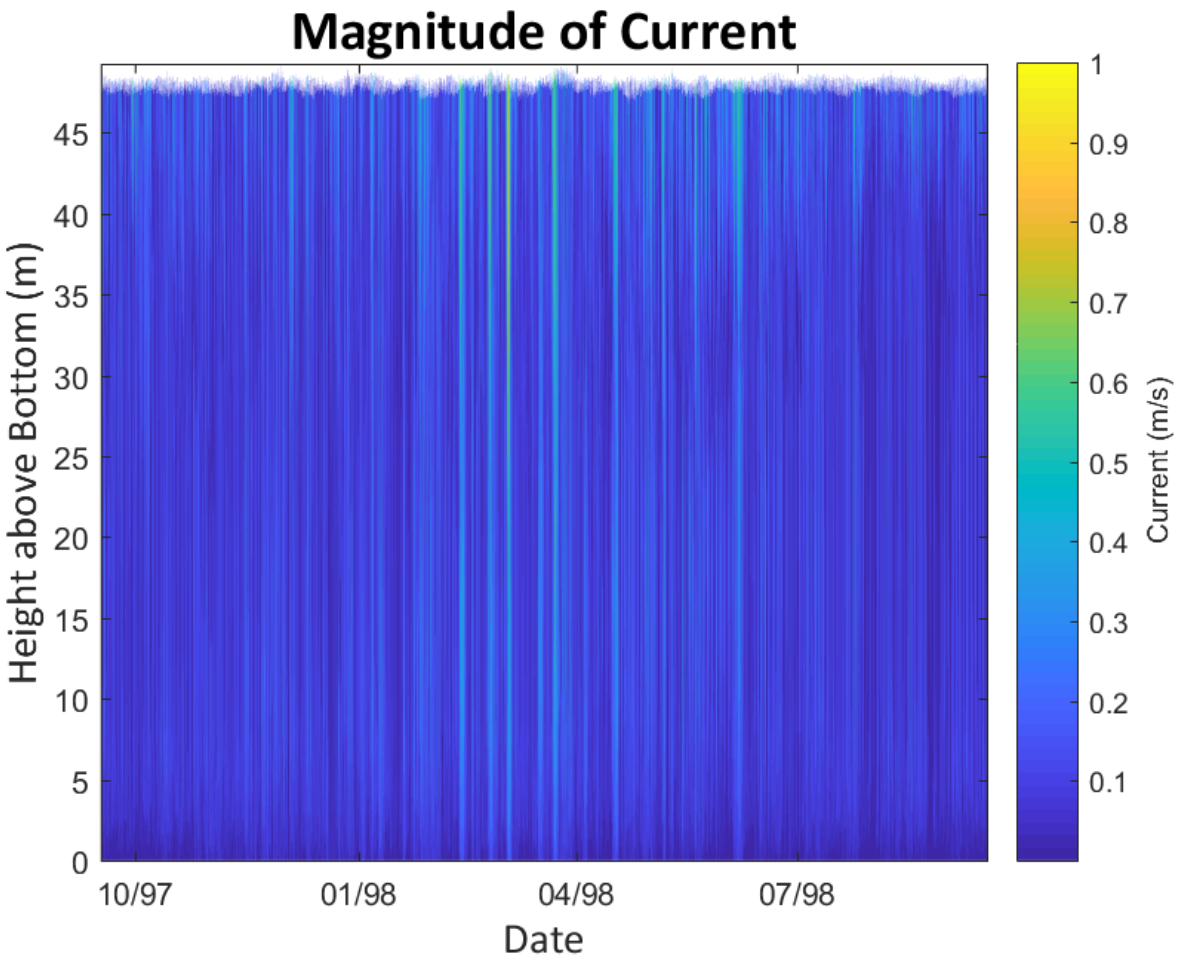

Figure 3-1. **NECOFS model results for currents, combined u and v components, near the proposed OCS-DC from September 17, 1997 through September 16, 1998.**

A review of the temperature simulations from the NECOFS model was also conducted to gain insight into seasonal and spatial variations in temperature as shown in Figure 3-2. Vertically, temperatures throughout the water column from the NECOFS model results exhibit minimal variation with an average difference between the surface and bottom layers of 0.036°F (0.02°C), and a measured maximum difference between the top and bottom layers of 0.504°F (0.28°C). Temporally, there is noticeable variation between the seasonal temperatures. For the purposes of this study, the four seasons were defined as follows: Fall consisted of the months September, October, and November; Winter consisted of December, January, and February; Spring was designated as March, April, and May; and Summer consisted of the months of June, July, and August. Mean temperatures were highest in the Fall and Summer months at 67.3°F (19.6°C) and 64.6°F (18.1°C), respectively, and much lower during Winter and Spring at 46.6°F (8.1°C) and 51.8°F (11.0°C).

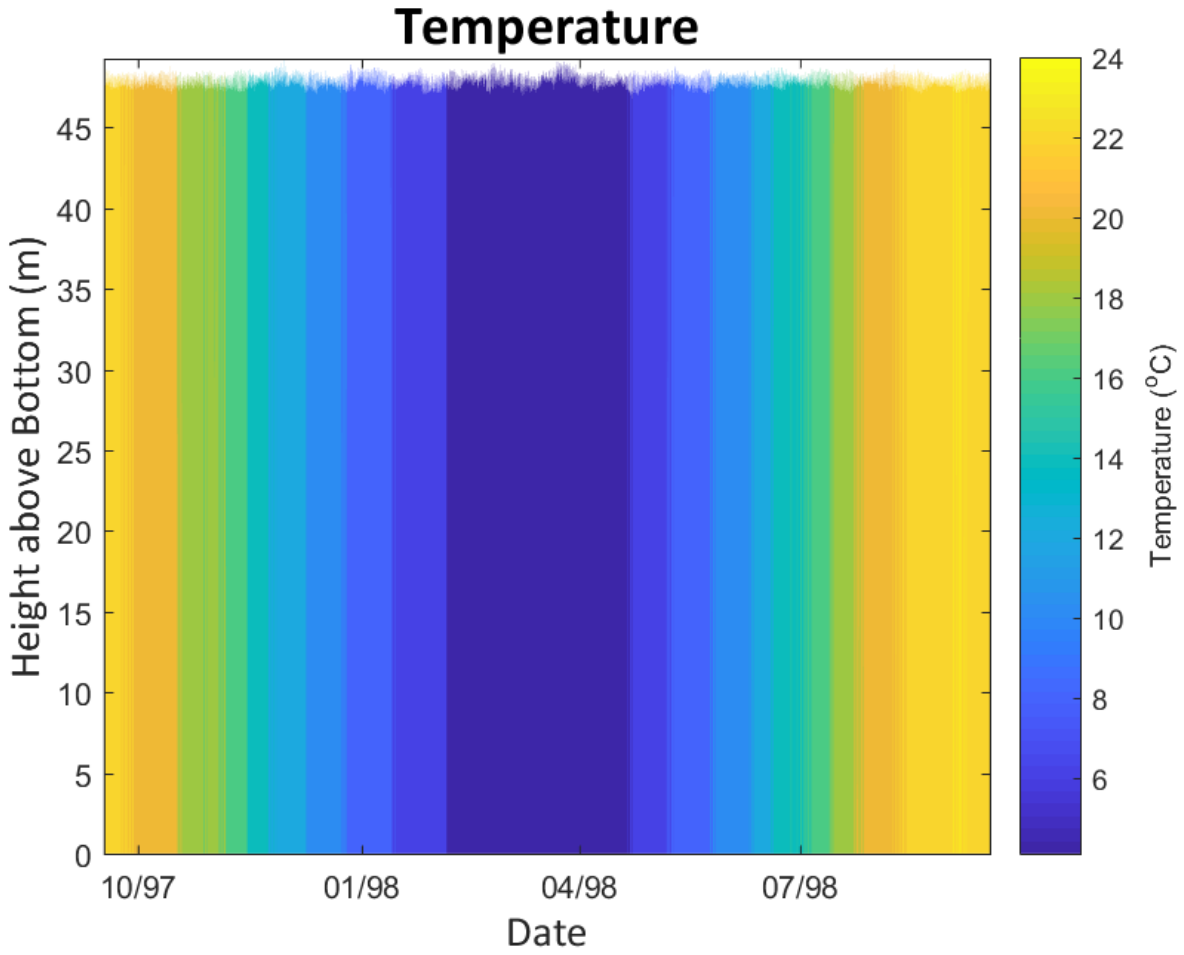

Figure 3-2. Contours of temperature in degrees Celsius from September 17, 1997 to September 16, 1998, near the proposed OCS-DC.

4.0 INTAKE HYDRAULIC ZONE OF INFLUENCE

To define the current field in the water column for determining the HZI associated with the intake pipes during water withdrawal, the current at each point in time was averaged over the depth of the water column to create the times series shown in Figure 4-1. As a conservative assumption for the analysis, the minimum depth-averaged current of 0.09 ft/s (0.026 m/s), shown on the figure (red circle), was used to develop the ambient flow field for determining the intake HZI shown in Figure 4-2. Currents in the water column at the time of the depth-averaged minimum ranged from as low as 0.016 ft/s (0.005 m/s) at 71.5 ft (21.8 m)) above the seabed to a maximum of 0.25 ft/s (0.075 m/s) at the free surface. The blue box in Figure 4-2 encapsulates the flow field from the ocean bed to the proposed intake height at 30 ft (10 m) above the bottom. At the 21.6 ft^2 (2.01 m^2) intake opening, the ambient current for the analyses was 0.66 ft/s (0.02 m/s) with a minimum of 0.046 ft/s (0.014 m/s) at 21.33 ft (6.5 m) above the seabed.

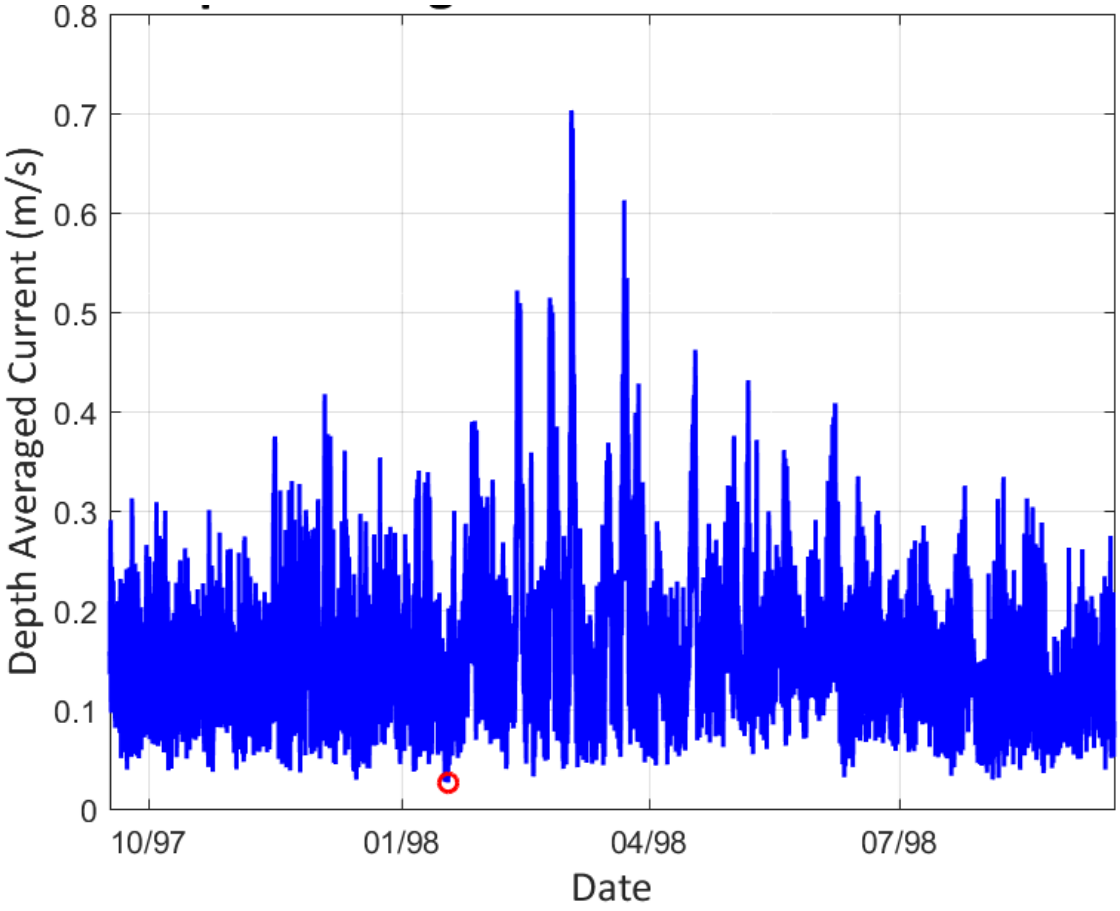

Figure 4-1. Time series of depth-averaged current during the average annual year. The red circle indicates the minimum current on January 17, 1998.

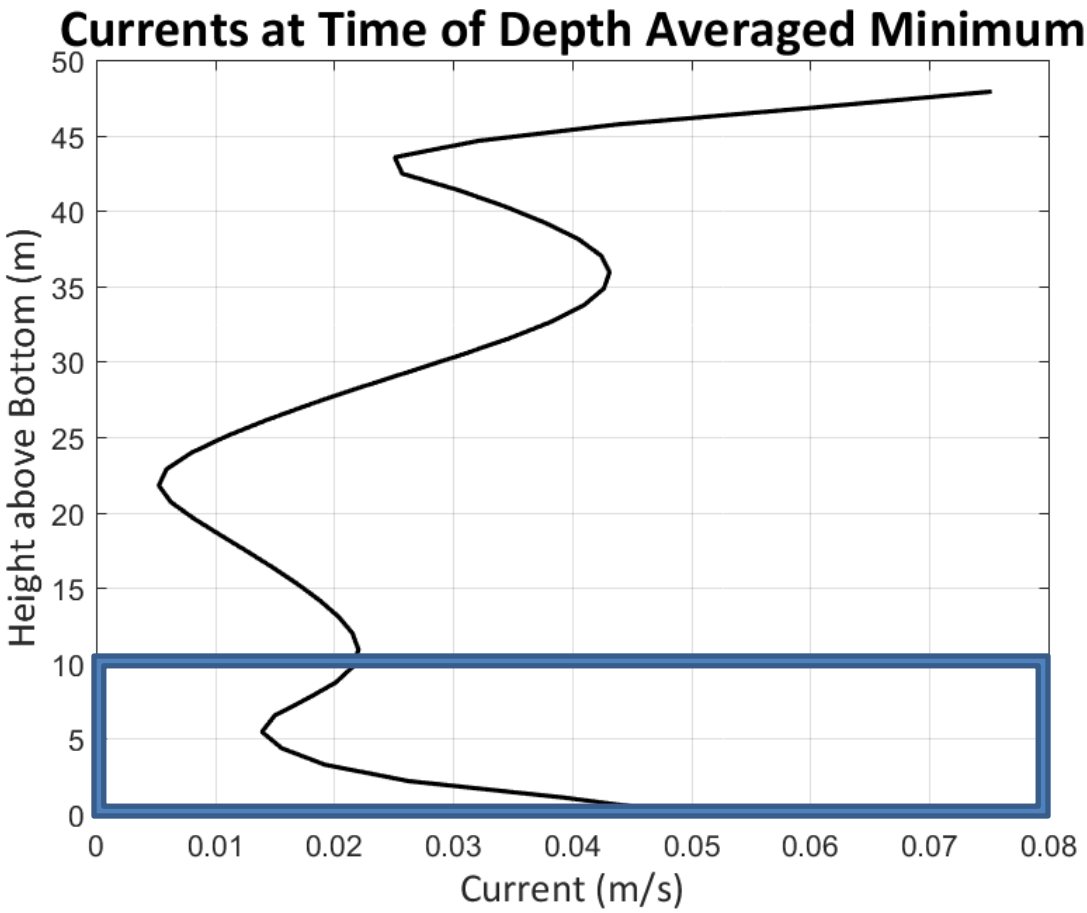

Figure 4-2. NECOFS currents at the time of the depth-averaged velocity minima throughout the water column. The blue box illustrates the portion of the water column between the seafloor and the proposed intake at 30 ft (10 m) above the bottom.

Stream function theory was used to develop both the ambient flow field and the flow field during withdrawals through the intake pipes. The velocities calculated using the stream functions were then summed to determine the combined flow field for both the existing ocean currents and the effects of the intake. In stream function theory, the flows are considered to be steady, irrotational plane flows such that the continuity equation can be reduced to:

$$\frac{\delta u}{\delta x} + \frac{\delta v}{\delta x} = 0 \quad Equation\ 2$$

Where *u* and *v* are the x- and y-components of the velocity which can be defined by a stream function ψ such that the individual components can be related by:

$$u = \frac{\delta \psi}{\delta y} \quad \& \quad v = \frac{\delta \psi}{\delta x} \quad Equation\ 3A\ \&\ 3B$$

A comprehensive discussion of stream function theory in cylindrical coordinates is provided in Appendix A.

Using the simulated currents output by the NECOFS model from January 17, 1998, a cross-sectional plot of streamlines, which indicate equal flow conveyance, was generated for the ambient flow field, and is shown in Figure 4-3. On the figure, streamlines that are spaced farther apart indicate lower currents, while those spaced closer together indicate higher currents.

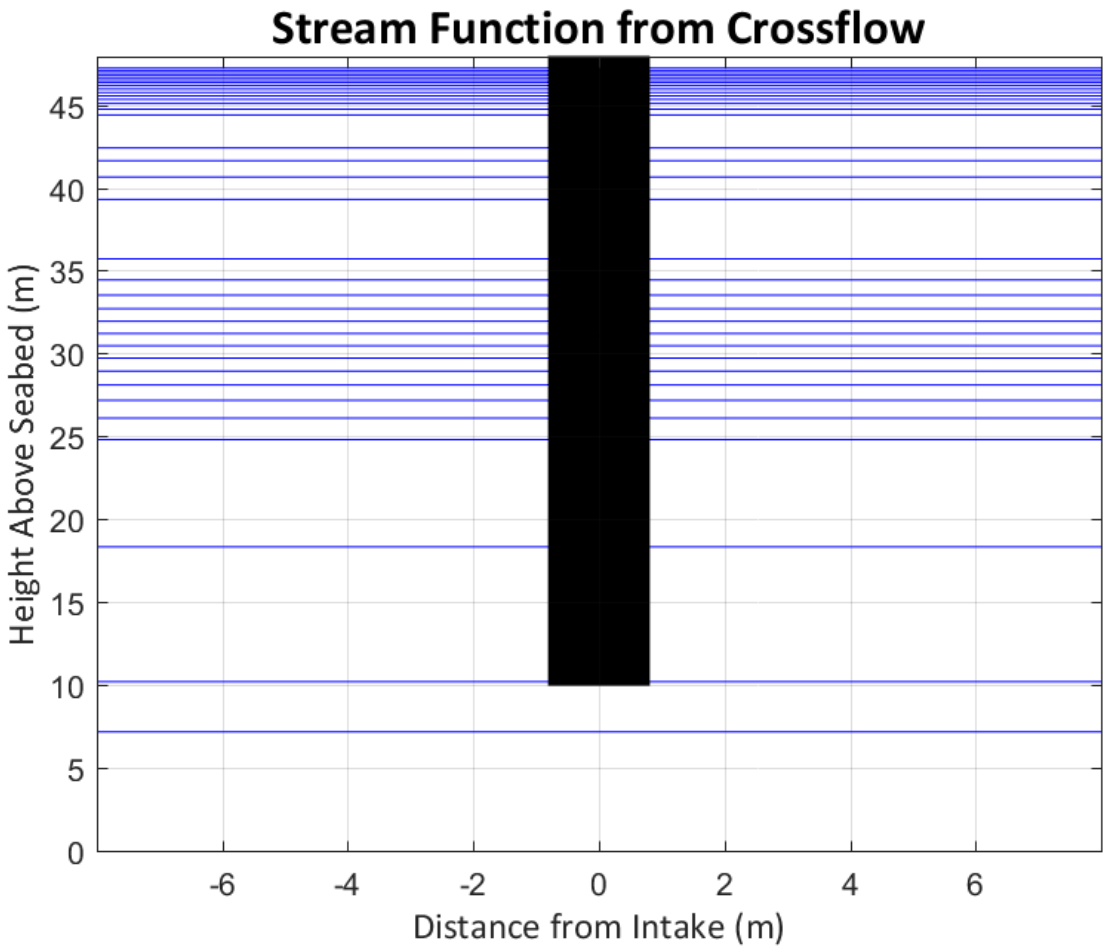

Figure 4-3. Stream function for the ambient flow field in the vicinity of the OCS-DC.

The stream function for the intake pipes during water withdrawal was calculated in a similar fashion but using cylindrical coordinates where the intake is considered (i.e., analytically defined) to be a line sink (flow removal) with a flow rate of 8.1 MGD (0.355 m^3/s) and a design intake velocity of 0.43 ft/s (0.13 m/s) per intake unit. In total, there are three intake pipes, however due to the close proximity to each other, the pipes were evaluated as a single line sink. The general form of the stream function for during the water withdrawal activity is given by the equation:

$$\psi = \frac{Q}{2\pi}\Theta \quad Equation\ 4$$

Where the vertical component of the velocity, *w*, is given by Equation 5A, and the radial component (v_r) is given by Equation 5B.

$$w = \frac{1}{r}\frac{\partial \psi}{\partial r} \ \& \ v_r = -\frac{1}{r}\frac{\partial \psi}{\partial z} \quad Equation\ 5A\ \&\ Equation\ 5B$$

Streamlines during water withdrawal activity are shown in Figure 4-4 where the greatest velocities occur near the intake pipe opening and reduce in magnitude with distance. As with the ambient current, the closer the streamlines are to each other, the higher the velocity as the streamlines represent "tubes" of equal flow conveyance.

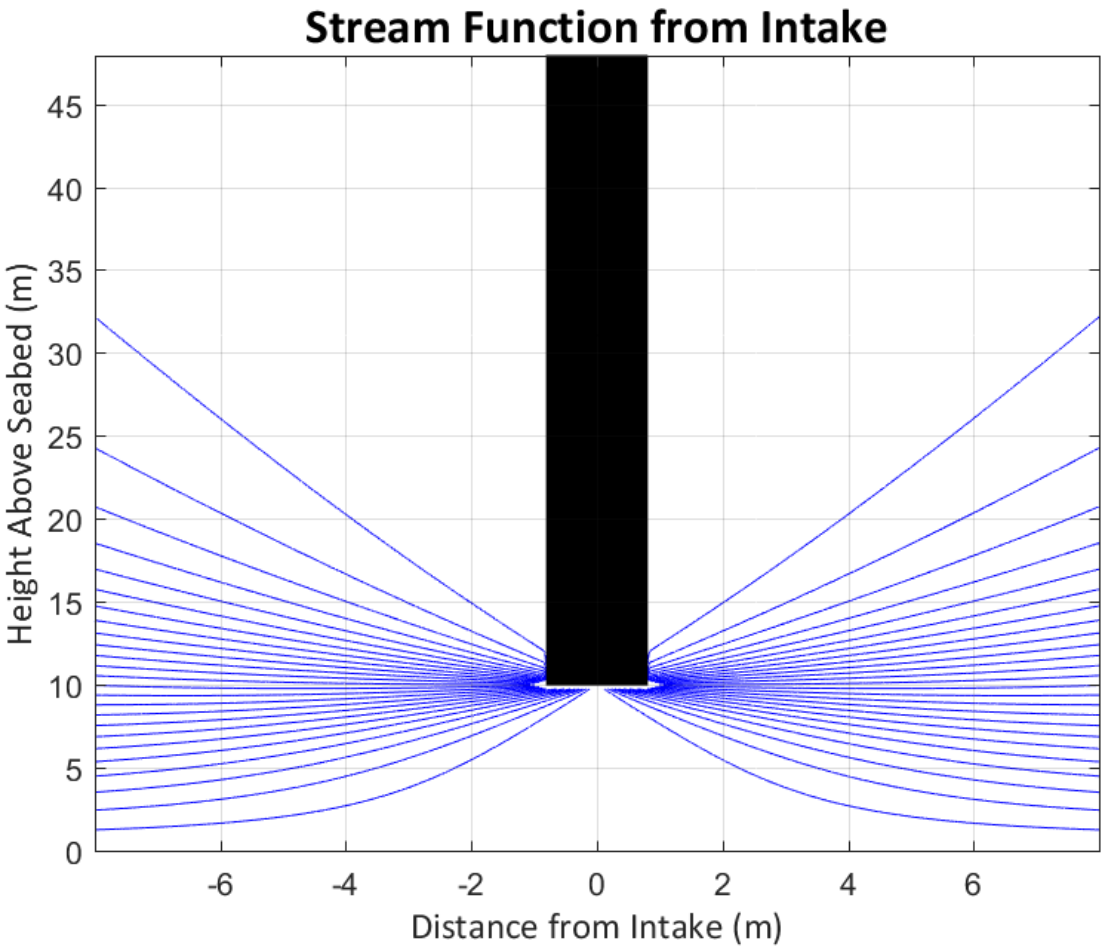

Figure 4-4. Stream function at the OCS-DC intake pipes during water withdrawals with a design entrance velocity of 0.13 m/s.

The flow rates during water withdrawal activity were calculated using the relationship of the stream function to the radial component of velocity (u_r) and vertical component of velocity (w) given in Equation 5A and Equation 5B, and were combined with the along-radius ambient velocity (u) to create a dimensionless current speed (U) by Equation 6, to generate the contours of current speed depicted in Figure 4-5. Other than localized currents in the immediate vicinity of the intake pipes, velocities influenced by the intake are on the order of tenths of a meter per second.

$$U = \sqrt{(u + u_r)^2 + w^2} \qquad Equation\ 6$$

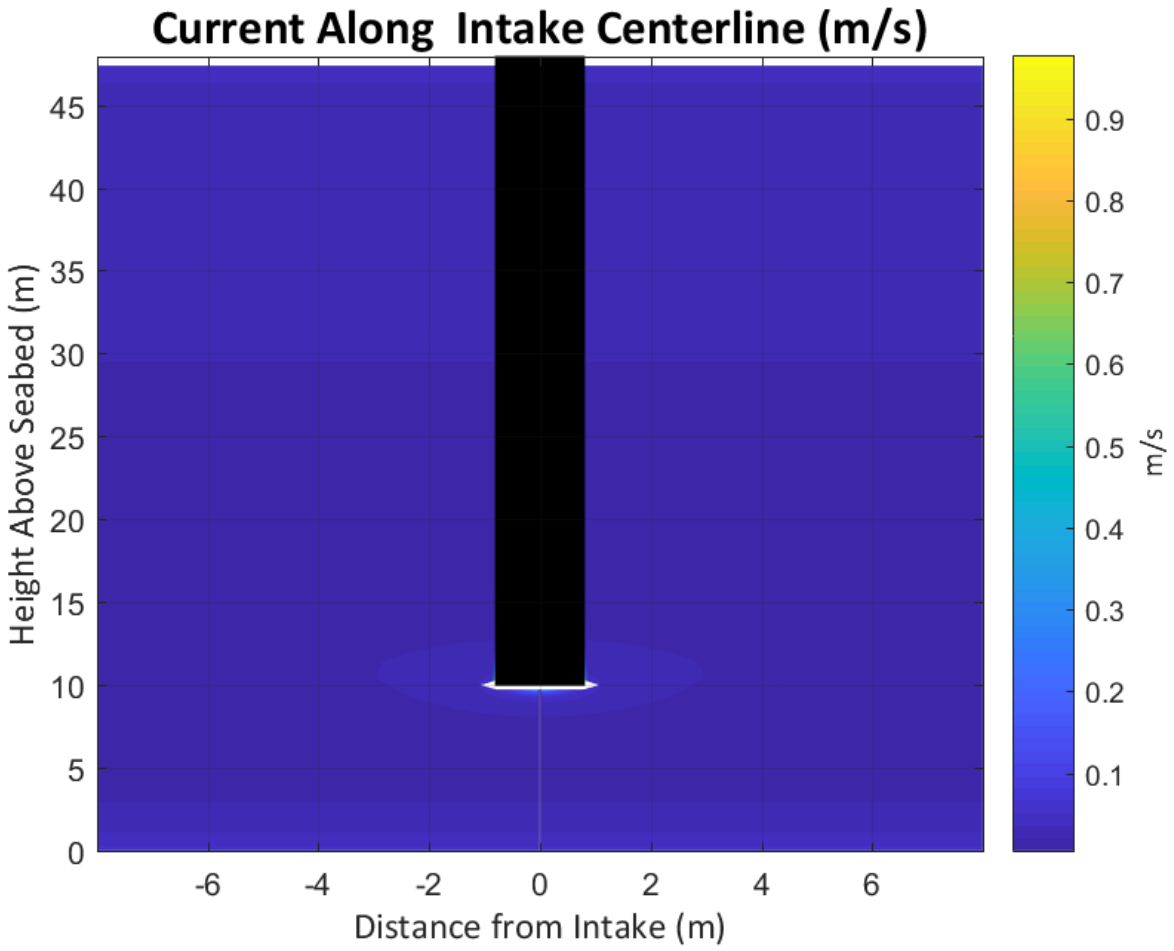

Figure 4-5. Combined flow field during OCS-DC water withdrawas and ambient currents.

Figure 4-6 shows a profile view, or vertical slice, of the changes in velocity due to water withdrawal activity as contours from 0% to 100% in 10% increments. To define the intake HZI local velocity changes of 10% (i.e., where the influence of the intake exceeds 10% of the normal ambient currents absent the intake) are shown as a red line in the figure. The 10% threshold was selected based on experience with similar studies. It reflects a reasonable threshold of influence considering the conservatively low magnitude of ambient current speeds used for this analysis (e.g., 0.09 ft/s per above), such that the threshold for the HZI is a quite low velocity of ~0.009 ft/s. An additional yellow line, representing the 5% change in velocity, is also shown on the figure to provide additional information on the effects of the intake flows on the ambient flow field. The 10% intake HZI extends radially from the structure for a distance of 12.1 ft (3.7 m), and to a depth of 18.8 ft (5.72 m) above the ocean floor. Extents of the 10% and 5% areas are also listed in Table 4-1. Neither the region encompassed by the 10% or even 5% HZI intersect the seafloor.

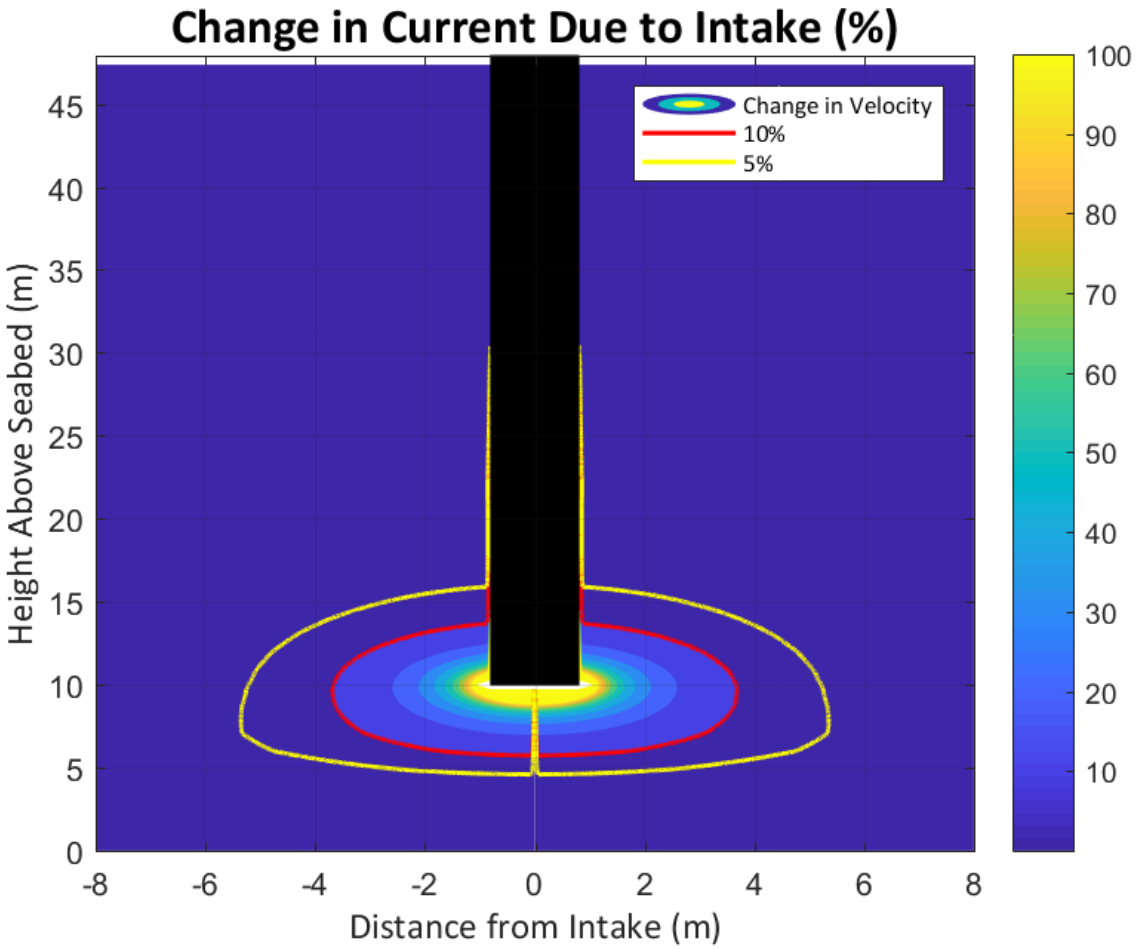

Figure 4-6. Profile view of the intake HZI. The red contour indicates a 10% increase over the ambient flow field, while the yellow contour indicates a 5% increase.

Table 4-1. Extent of the CWIS HZI.

	Radial Distance from Intake	Minimum Height above Bottom	Area
10 % Increase	3.70 m (12.13 ft)	5.72 m (18.76 ft)	43.03 m^2 (463.17ft^2)
5 % Increase	5.27 m (17.29 ft)	4.59 m (15.06 ft)	87.11 m^2 (937.64 ft^2)

Figure 4-7 shows a plan view of the same information showing a different perspective of the intake structure's effect on the ambient currents as colored contours. In this figure, the maximum change at any point in the water column as shown as a horizontal slice at a given height above the seabed. The extent of the 10% change is also shown on the figure as a solid red line with radius of 12.1 ft (3.7 m), and an additional contour, shown in yellow, represents the extents of the 5% change with radius of 17.3 ft (5.27 m) in current radially about the intake structure.

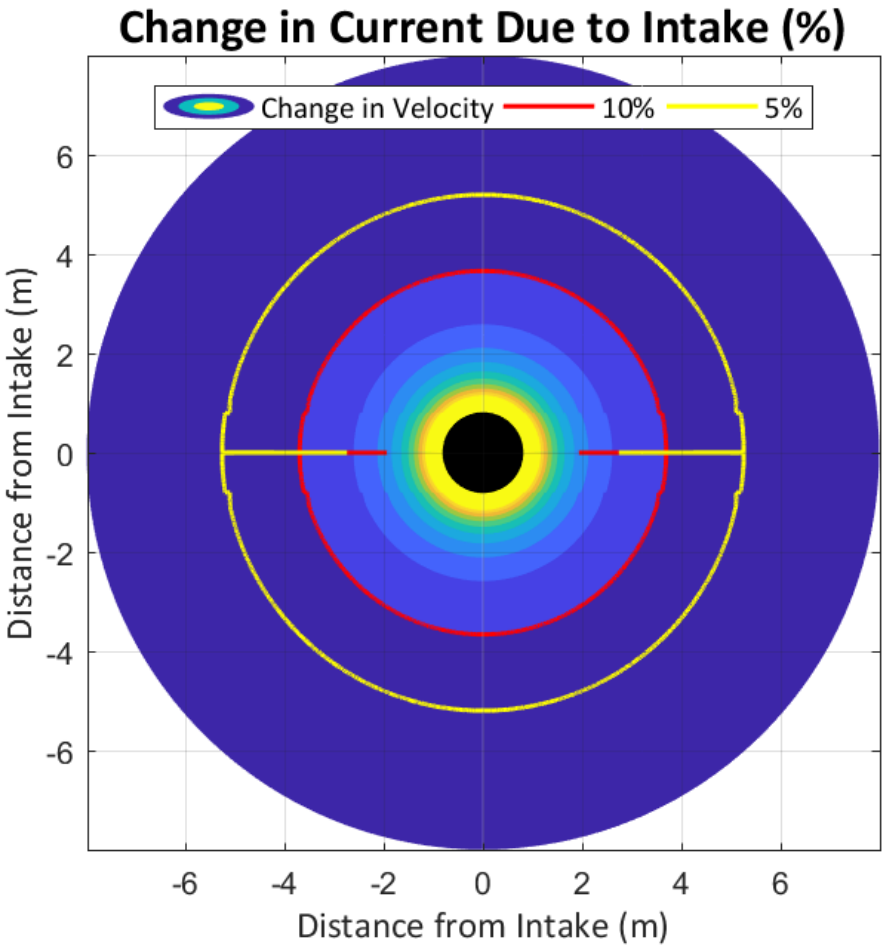

Figure 4-7. Plan view of the intake HZI.

5.0 OUTFALL THERMAL PLUME

For the purposes of this assessment, all of the water withdrawn through the intake pipes is used for cooling heat exchange equipment and then discharged at an elevated temperature back to the source water through the Dump Caisson. Three potential design alternatives for the discharge configuration were evaluated: 1) a single point source discharge at a depth of 18 ft (6 m) below LMSL, 2) a single point discharge located approximately 40 ft (12 m) below LMSL, and 3) a single point discharge located 100 ft (30 m) below LMSL. In all scenarios, the total area of the Dump Caisson was 5.4 ft^2 (0.5 m^2).

To gain understanding of the extents of the thermal plume, the CORnell MIXing Zone Expert System (CORMIX) was selected to simulate dilution of the heated discharge. CORMIX is a widely accepted Environmental Protection Agency-approved mixing zone model capable of determining both near-field and far-field thermal plume behavior in both steady and unsteady (tidal) environments (Doneker & Jirka, 2007). Because of the tidal component of the ambient currents, CORMIX simulations used the unsteady flow module for a submerged environment. Due to the seasonal variability of the sound for both temperature and ambient currents, the NECOFS data was subdivided into four seasonal bins:

1. Fall consisting of the months of September, October, and November,
2. Winter consisting of the months of December January, and February,
3. Spring consisting of the months of March, April, and May, and
4. Summer consisting of the months of June, July, and August.

For each seasonal bin, the lowest observed temperature during that time period was selected to represent the most conservative temperature differential (ΔT) between ambient conditions and the thermal effluent. The CORMIX model can account for additional heat dissipation using a surface heat exchange coefficient, in W/m^2 °C, and additional wind-induced turbulent mixing using an ambient wind speed; however, both values were specified as 0 to add additional layers of conservatism for this analysis. These more complex processes can sometimes necessitate a hydrodynamic far-field model if substantial thermal influences extend beyond the near-field. In the simulations, the ambient water depth was specified at 154.2 ft (46 m), and a Manning's n roughness coefficient of 0.018 consistent with a clean, earthen channel (Chow, 1959). Seasonal velocities for each scenario were calculated by demeaning the velocities for each season, and calculating the average of peaks, which were then used with the corresponding seasonal low temperatures listed in Table 5-1 as inputs to CORMIX.

Table 5-1. Ambient water body characteristics used for CORMIX modeling of thermal plume behavior in the Near Field Region (NFR).

Season	Temperature	Current at 6m (18 ft)	Current at 12m (40 ft)	Current at 30m (100 ft)
Fall	13.2 °C (55.76°F)	0.261 m/s (0.86 ft/s)	0.218 m/s (0.72 ft/s)	0.208 m/s (0.68 ft/s)
Winter	4.6 °C (40.28 °F)	0.294 m/s (0.96 ft/s)	0.256 m/s (0.84 ft/s)	0.243 m/s (0.80 ft/s)
Spring	4.1 °C (39.38 °F)	0.334 m/s (1.10 ft/s)	0.273 m/s (0.90 ft/s)	0.277 m/s (0.91 ft/s)
Summer	10.6 °C (51.08 °F)	0.264 m/s (0.87 ft/s)	0.207 m/s (0.68 ft/s)	0.214 m/s (0.70 ft/s)

5.0.1 Thermal Plume at 6 Meters Below Local Mean Sea Level

Using the 12.4-hour period semidiurnal tide, simulations for each season were simulated at 3.1 hours before and after slack tide to provide the largest combination of ambient currents and time before flow reversal to allow the plume to propagate with the prevailing currents in the receiving water body. This period in the tide results in conditions that would advect the thermal plume furthest from the Dump Caisson. The Dump Caisson was assumed to be discharging vertically downward into the ambient water column through the 5.4 ft^2 (0.5 m^2) opening. To define the extent of the thermal plume (i.e., mixing zone), a 1°C ΔT above ambient was specified. For each simulation, the 1°C ΔT threshold was met within the NFR simulated by CORMIX where turbulent mixing of the heated discharge is the dominant mechanism for heat dispersal. This result strengthens confidence in using CORMIX for this application. The extents of the thermal plume above the 1°C ΔT threshold for each scenario are listed in Table 5-2. Plan and profile plots of the thermal plume in the NFR are shown for each scenario in Figure 5-1 through Figure 5-4. In these figures the red contour shows the extent of the plume with a temperature difference greater than 1°C, while the black line shows the 4°C ΔT.

At the farthest ends of the NFR for the 18 ft (6m) discharge depth, the thermal plume changes behavior and shape, as the turbulent mixing no longer dominates plume behavior and advection and spreading become more important to plume behavior, resulting in a plume of uniform temperature, width, and height. The 1°C isotherm in this section of the mixing zone can extend from the surface of the water to a depth of up to 13.1 ft (4.0 m), and can be as much as 14.8 ft (4.5 m) wide.

Table 5-2. Thermal plume extent above a 1°C ΔT NFR for 6m below LMSL.

	3.1 Hours Before Slack			3.1 Hours After slack		
Season	**Length**	**Width**	**Area**	**Length**	**Width**	**Area**
Fall	18.2 m (59.7 ft)	2.86 m (9.4 ft)	38.9 m^2 (419 ft^2)	18.5 m (60.7 ft)	3.1 m (10.2 ft)	43.4 m^2 (467 ft^2)
Winter	19.6 m (64.3 ft)	4.51 m (14.8 ft)	48.6 m^2 (523 ft^2)	19.6 m (64.3 ft)	4.51 m (14.8 ft)	48.6 m^2 (523 ft^2)
Spring	21.3 m (69.9 ft)	3.54 m (11.6 ft)	52.5 m (565 ft^2)	22.0 m (72.2) ft	4.21 m (13.8 ft)	55.9 m^2 (602 ft^2)
Summer	17.7 m (58.1 ft)	3.41 m (11.2 ft)	43.1 m^2 (464 ft^2)	17.7 m (58.1 ft)	3.41 m (11.2 ft)	43.8 m^2 (471 ft^2)

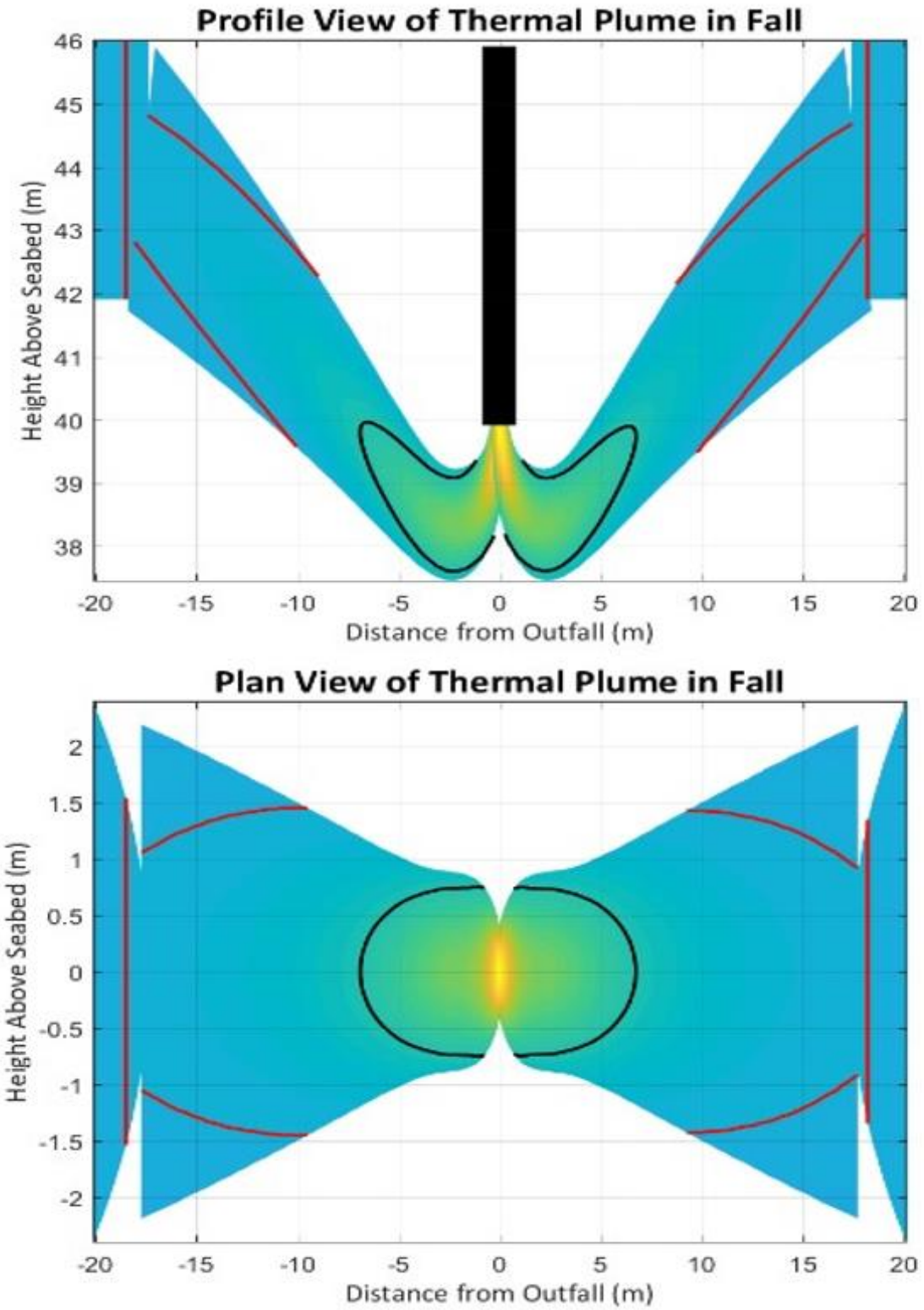

Figure 5-1. Profile view (top) and plan view (bottom) of the 6 m LMSL thermal plume in the NFR during fall.

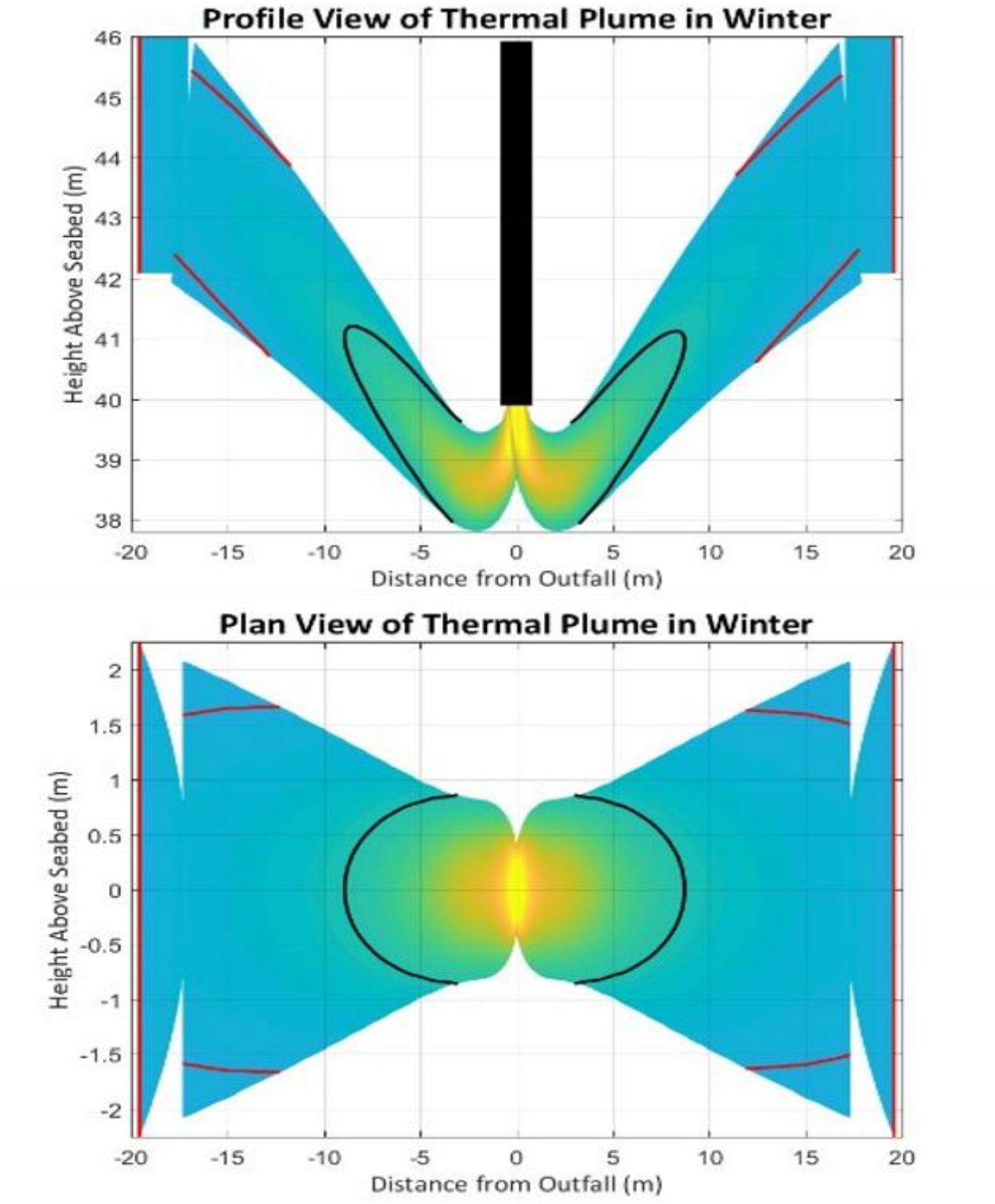

Figure 5-2. Profile view (top) and plan view (bottom) of the 6 m LMSL thermal plume in the NFR during winter.

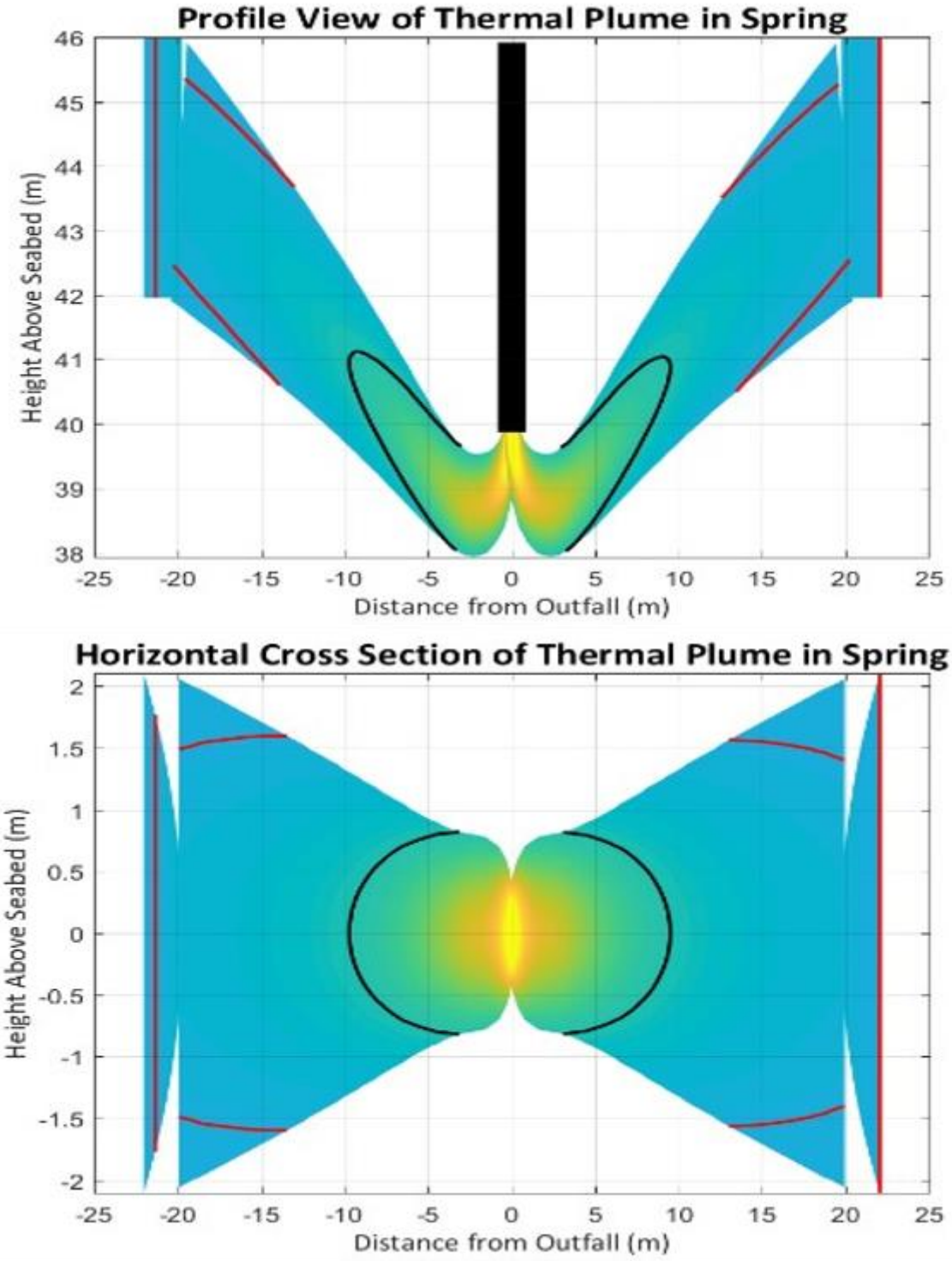

Figure 5-3. Profile view (top) and plan view (bottom) of the 6 m LMSL thermal plume in the NFR during spring.

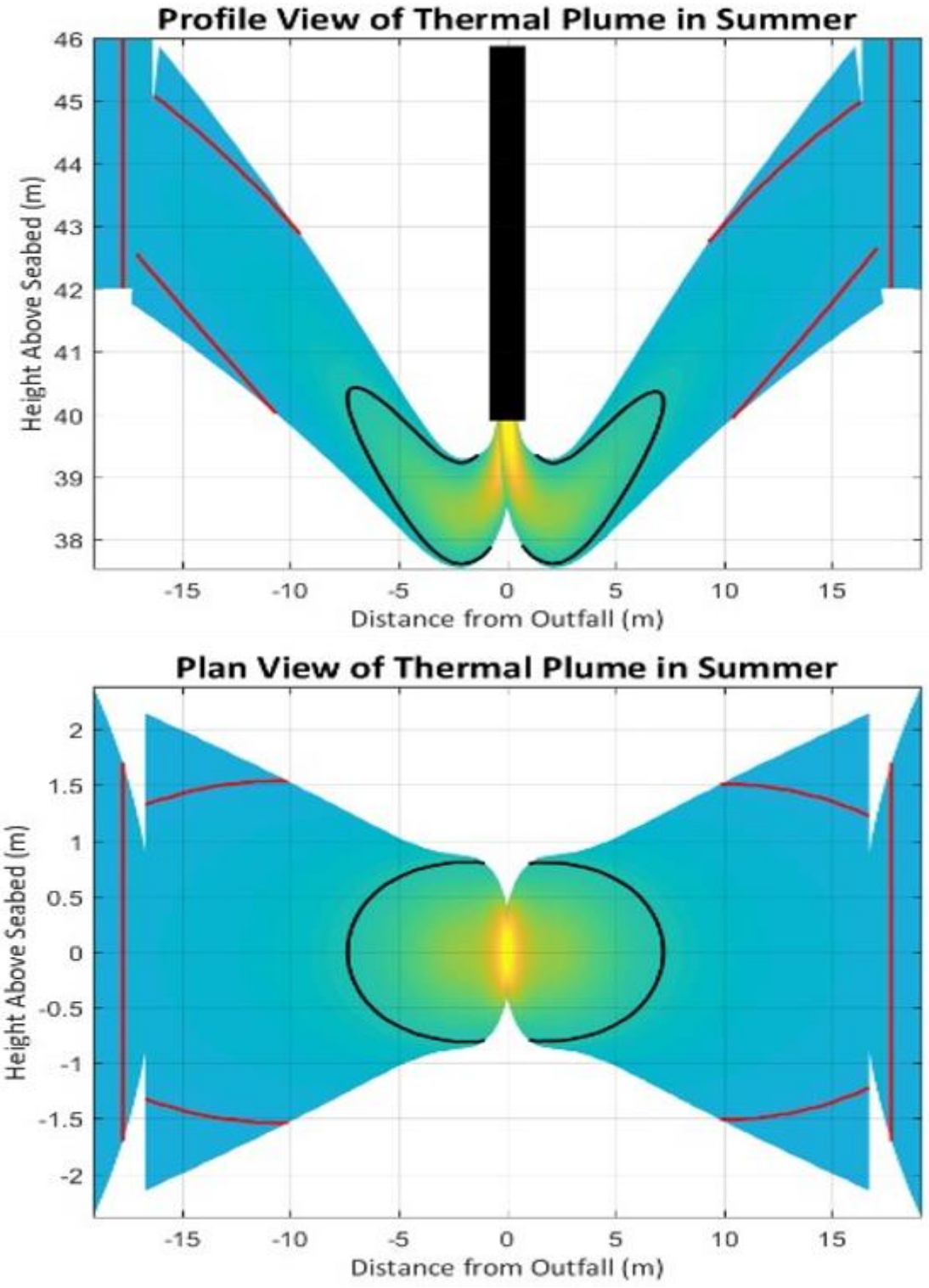

Figure 5-4. Profile view (top) and plan view (bottom) of the 6 m LMSL thermal plume after slack tide in the NFR during summer.

5.0.2 Thermal Plume at 12 Meters Below Local Mean Sea Level

Using the 12.4-hour period semidiurnal tide, simulations for each season were simulated at 3.1 hours before and after slack tide to provide the largest combination of ambient currents and time before flow reversal to allow the plume to propagate with the prevailing currents in the receiving water body. This period in the tide results in conditions that would advect the thermal plume furthest from the Dump Caisson. As with the previous scenario, the heated water was assumed to be discharged vertically downward. To define the extent of the thermal plume (i.e., mixing zone), a 1°C ΔT above ambient was specified. For each simulation, the 1°C ΔT threshold was met within the NFR simulated by CORMIX where turbulent mixing of the heated discharge is the dominant mechanism for heat dispersal. This result strengthens confidence in using CORMIX for this application. The extents of the thermal plume above the 1°C ΔT threshold for each scenario are listed in Table 5-3. Plan and profile plots of the thermal plume in the NFR are shown for each scenario in Figure 5-5 through Figure 5-8. In these figures the red contour shows the extent of the plume with a temperature difference greater than 1°C, while the black line shows the 4°C ΔT. The currents and temperatures for the 40 ft (12m) depth discharge are such that the 1°C isotherm is located entirely in the fully turbulent portion of NFR.

Table 5-3. Thermal plume extent above a 1°C ΔT NFR for 12 m below LMSL.

	3.1 Hours Before Slack			3.1 Hours After slack		
Season	**Length**	**Width**	**Area**	**Length**	**Width**	**Area**
Fall	17.42 m (57.15 ft)	3.02 m (9.91 ft)	40.90 m^2 (440.25 ft^2)	15.32 m (50.26 ft)	3.29 m (10.79 ft)	38.63 m^2 (415.79 ft^2)
Winter	23.55 m (77.26 ft)	3.44 m (11.29 ft)	59.88 m^2 (644.53 ft^2)	24.76 m (81.23 ft)	3.51 m (11.52 ft)	65.17m^2 (701.49 ft^2)
Spring	24.36 m (79.92 ft)	3.36 m (11.02 ft)	61.90 m^2 (666.29 ft^2)	26.32 m (86.35 ft)	3.44 m (11.29 ft)	66.90 m^2 (730.91 ft^2)
Summer	17.94 m (58.86 ft)	3.26 m (10.70 ft)	44.69 m^2 (480.99 ft^2)	18.96 m (62.20 ft)	3.33 m (10.93 ft)	48.11 m^2 (517.81 ft^2)

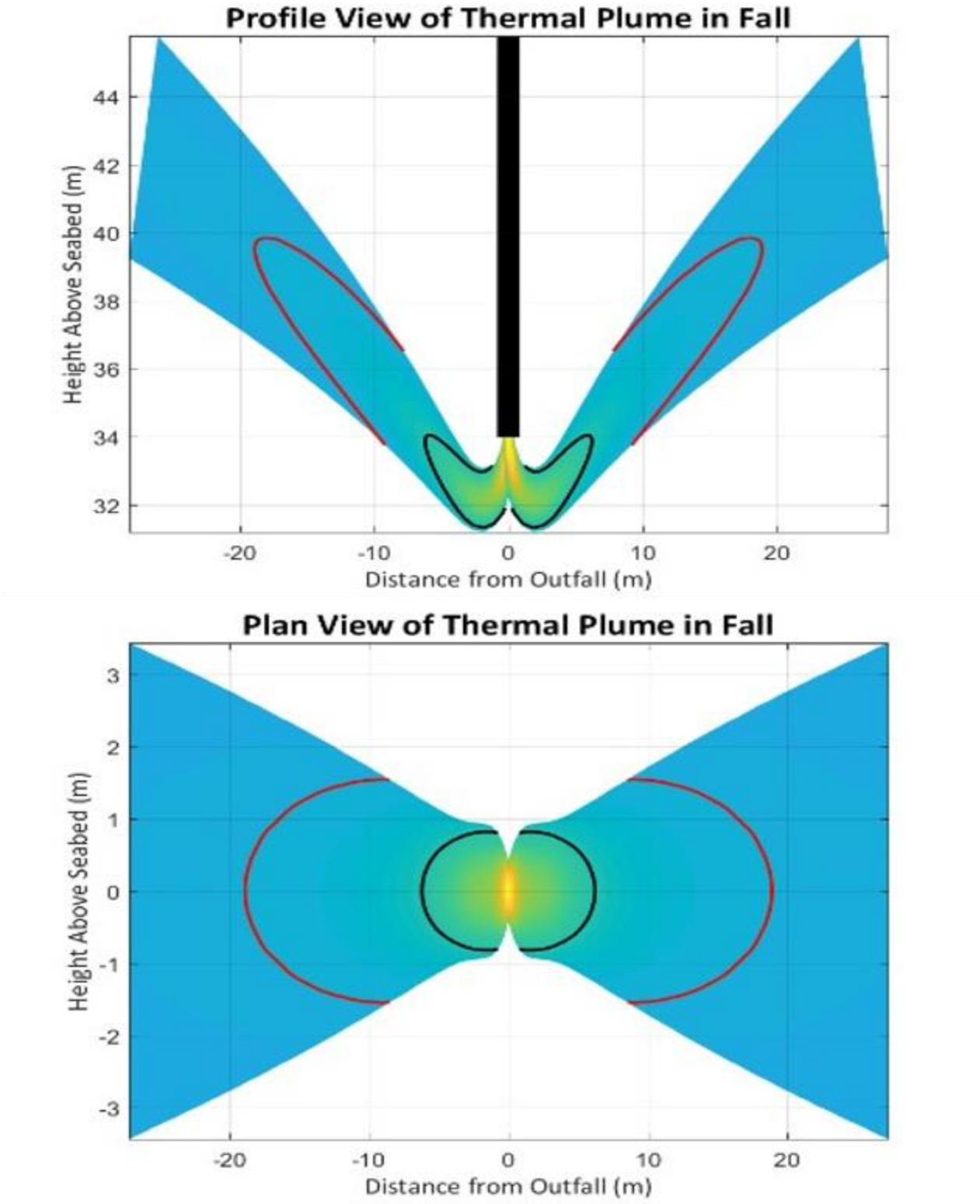

Figure 5-5. Profile view (top) and plan view (bottom) of the 12 m LMSL thermal plume in the NFR during fall.

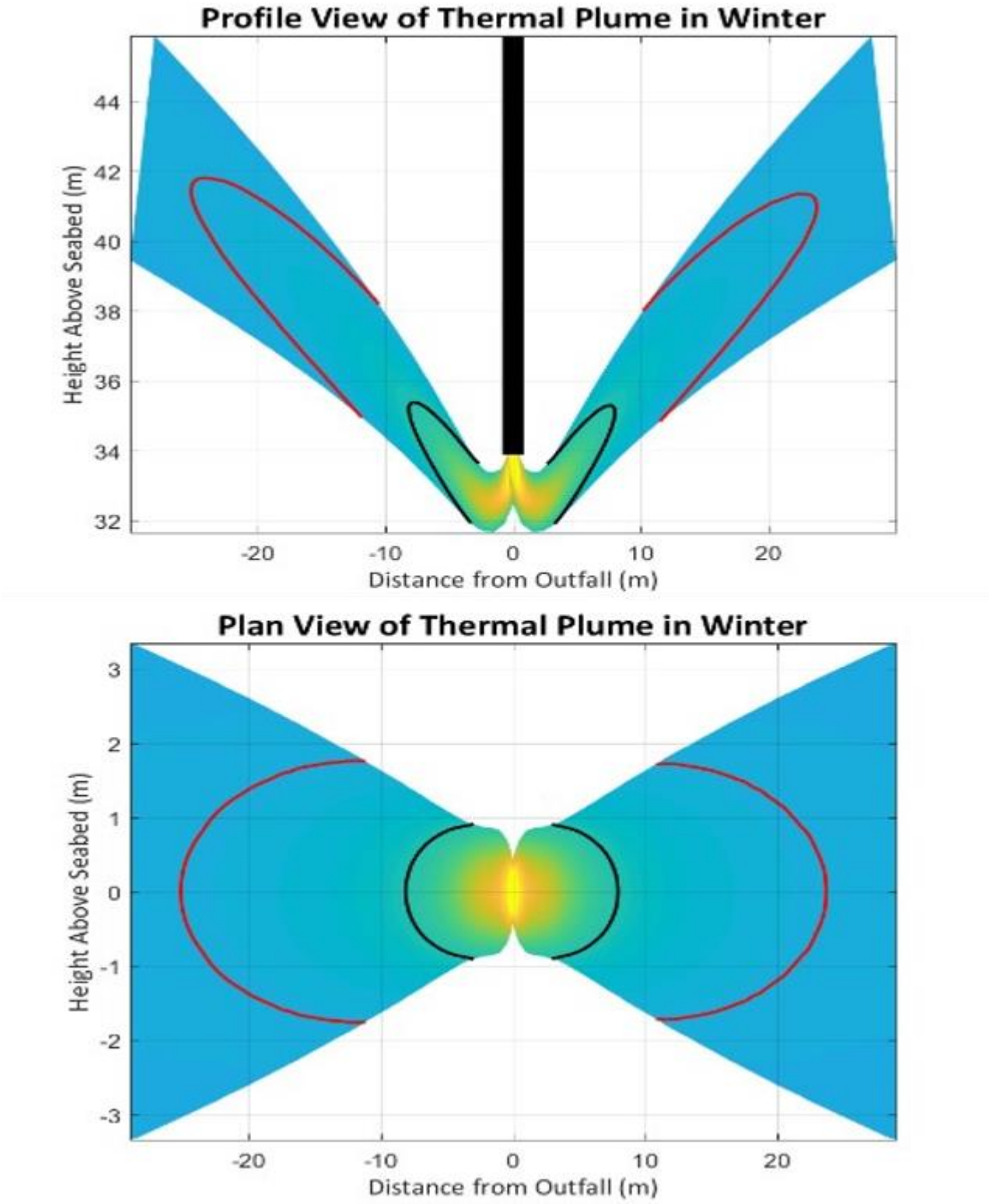

Figure 5-6. Profile view (top) and plan view (bottom) of the 12 m LMSL thermal plume in the NFR during winter.

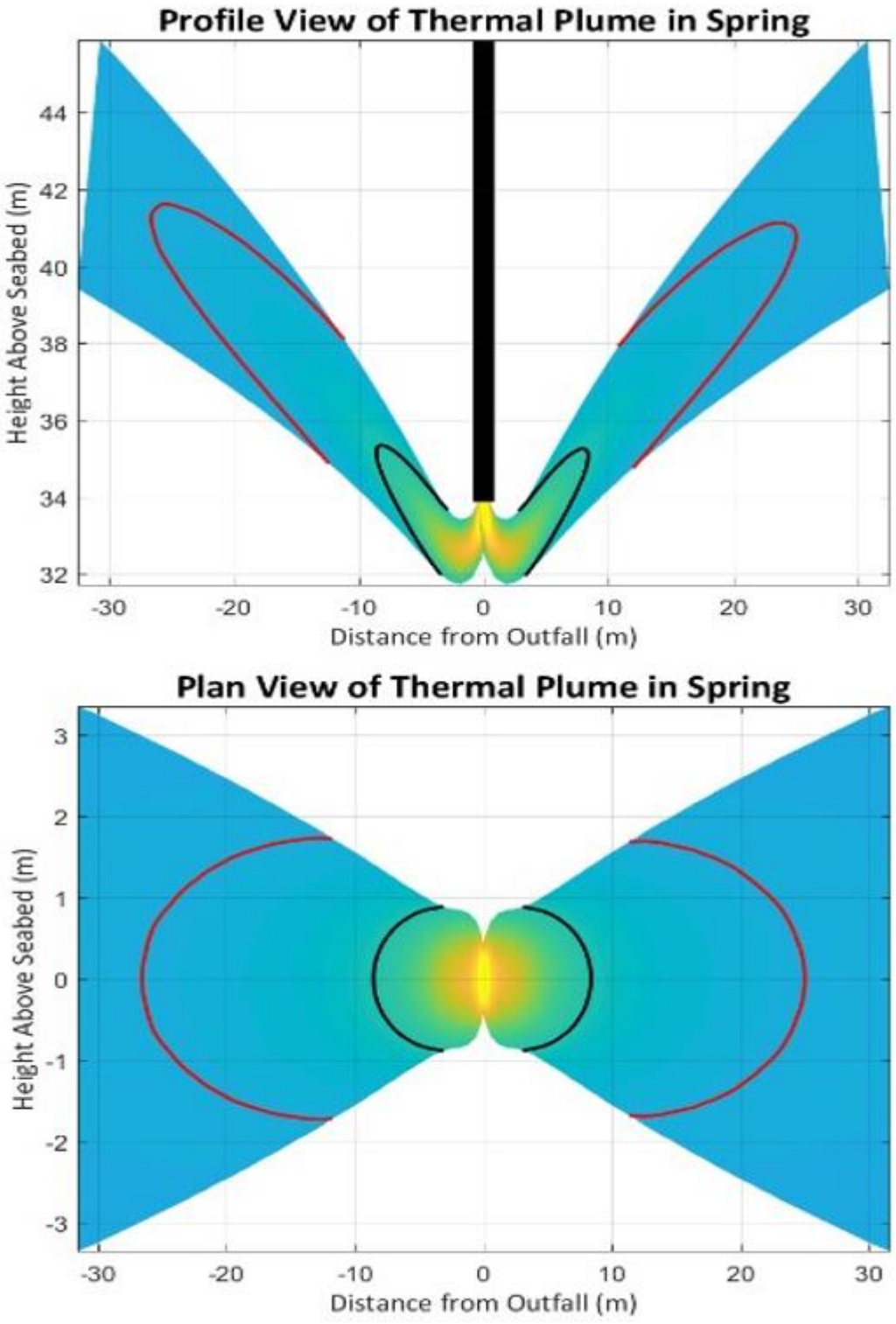

Figure 5-7. Profile view (top) and plan view (bottom) of the 12 m LMSL thermal plume in the NFR during spring.

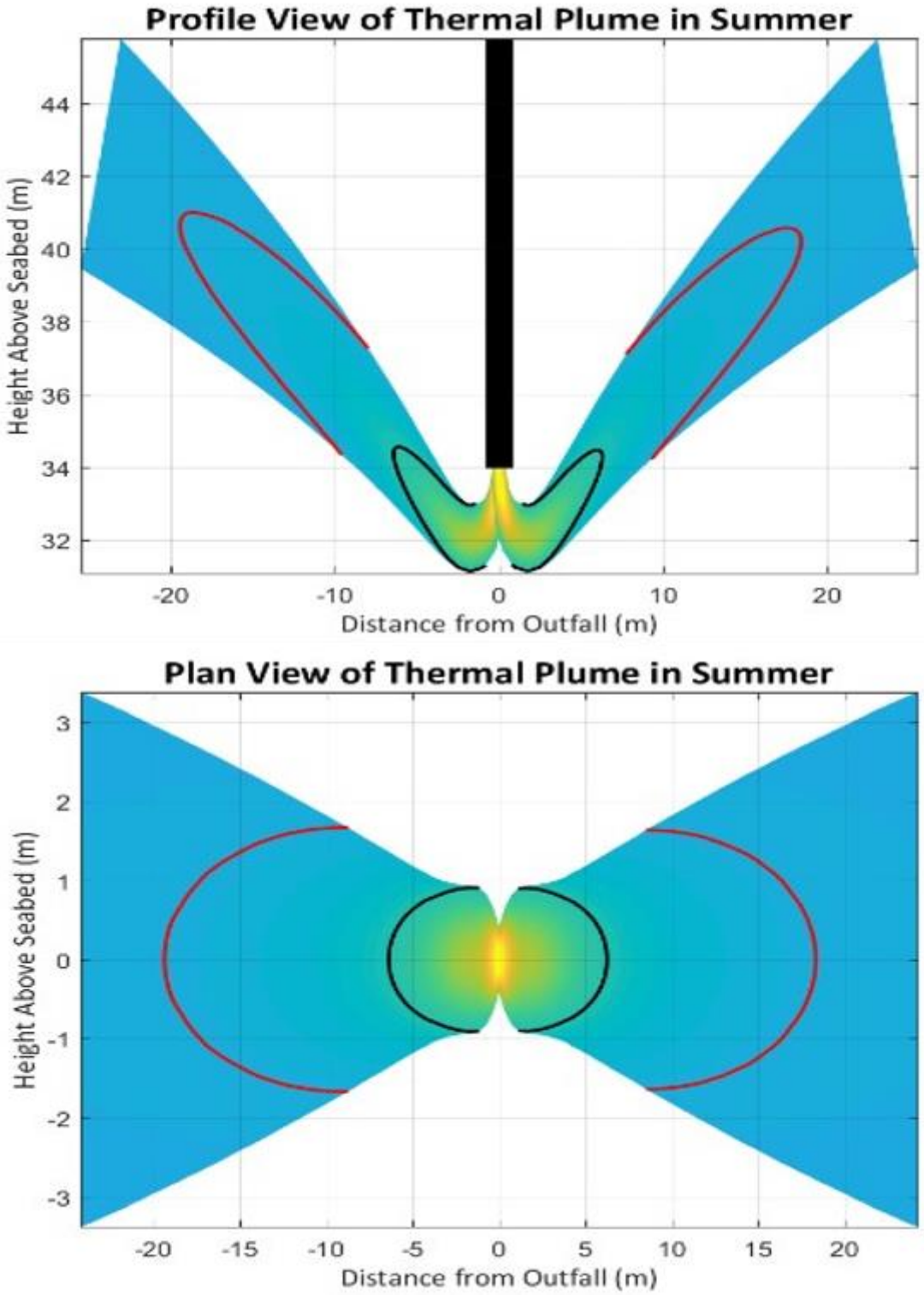

Figure 5-8. Profile view (top) and plan view (bottom) of the 12 m LMSL thermal plume after slack tide in the NFR during summer.

5.0.3 Thermal Plume at 30 Meters Below Local Mean Sea Level

Using the 12.4-hour period semidiurnal tide, simulations for each season were simulated at 3.1 hours before and after slack tide to provide the largest combination of ambient currents and time before flow reversal to allow the plume to propagate with the prevailing currents in the receiving water body. This period in the tide results in conditions that would advect the thermal plume furthest from the Dump Caisson. To define the extent of the thermal plume (i.e., mixing zone), a 1°C ΔT above ambient was specified. In the 100 ft (30 m) discharge depth, proximity to the seabed necessitated simulating the heated water being discharged vertically upwards towards the free surface. For each simulation, the 1°C ΔT threshold was met within the NFR simulated by CORMIX where turbulent mixing of the heated discharge is the dominant mechanism for heat dispersal. This result strengthens confidence in using CORMIX for this application. The extents of the thermal plume above the 1°C ΔT threshold for each scenario are listed in Table 5-4. Plan and profile plots of the thermal plume in the NFR are shown for each scenario in Figure 5-9 through Figure 5-12. In these figures the red contour shows the extent of the plume with a temperature difference greater than 1°C, while the black line shows the 4°C ΔT.

Table 5-4. Thermal plume extent above a 1°C ΔT NFR at 30 m below LMSL.

	3.1 Hours Before Slack			3.1 Hours After slack		
Season	**Length**	**Width**	**Area**	**Length**	**Width**	**Area**
Fall	12.50 m (41.0 ft)	2.95 m (9.68 ft)	29.3 m^2 (316 ft^2)	13.6 m (44.7 ft)	2.96 m (9.70 ft)	32.0 m^2 (344 ft^2)
Winter	15.1 m (49.5 ft)	3.84 m (12.6 ft)	43.9 m^2 (472 ft^2)	16.3 m (53.4 ft)	3.95 m (13.0 ft)	48.6 m^2 (524 ft^2)
Spring	20.4 m (67.0 ft)	3.25 m (10.6 ft)	51.7 m^2 (556 ft^2)	22.5 m (73.8 ft)	3.32 m (10.9 ft)	56.9 m^2 (613 ft^2)
Summer	14.95 m (49.0 ft)	3.13 m (10.3 ft)	34.8 m^2 (375 ft^2)	154.95 m (49.0 ft)	10.3 m (10.3 ft)	37.5 m^2 (404 ft^2)

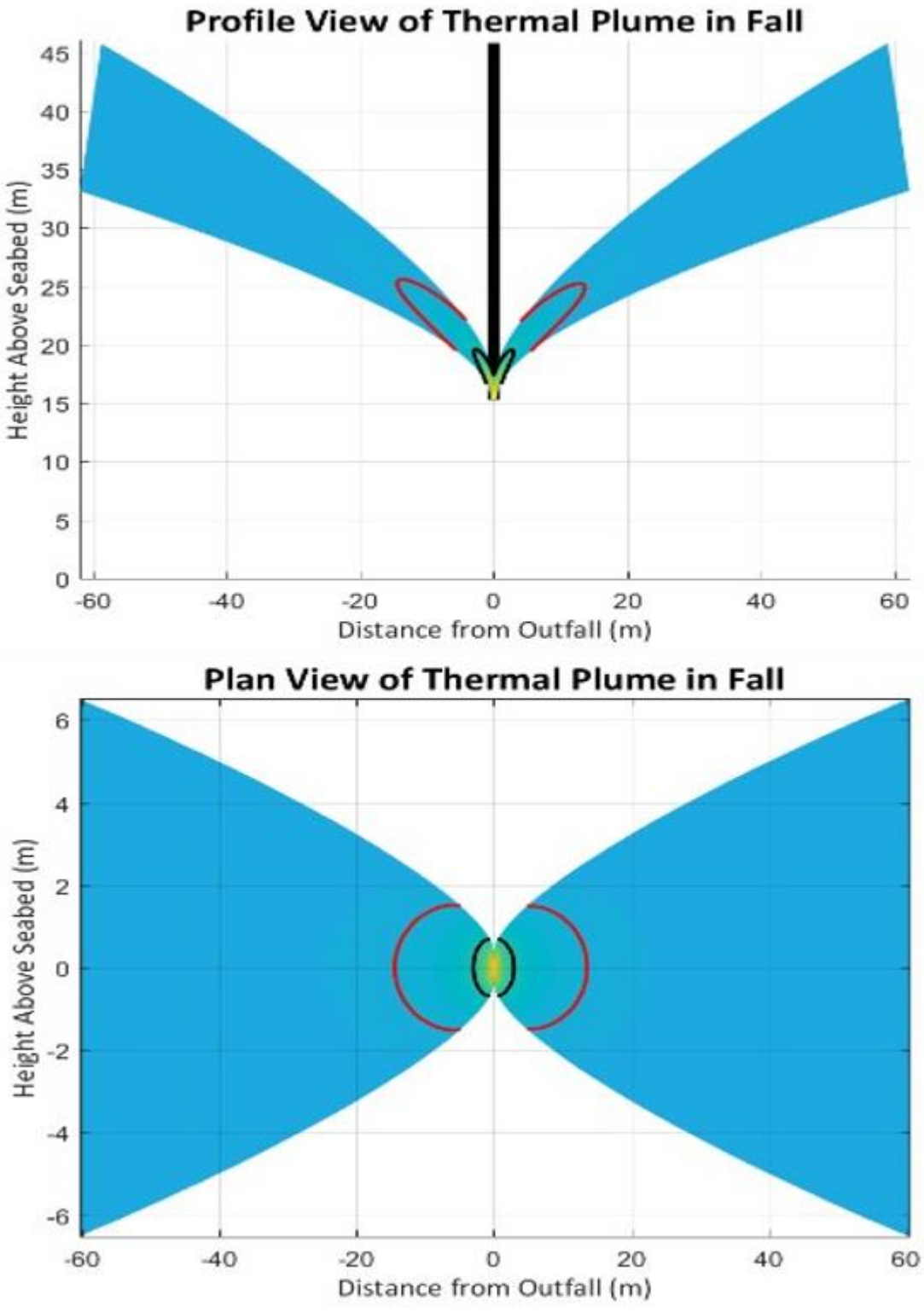

Figure 5-9. Profile view (top) and plan view (bottom) of the 30 m LMSL thermal plume in the NFR during fall.

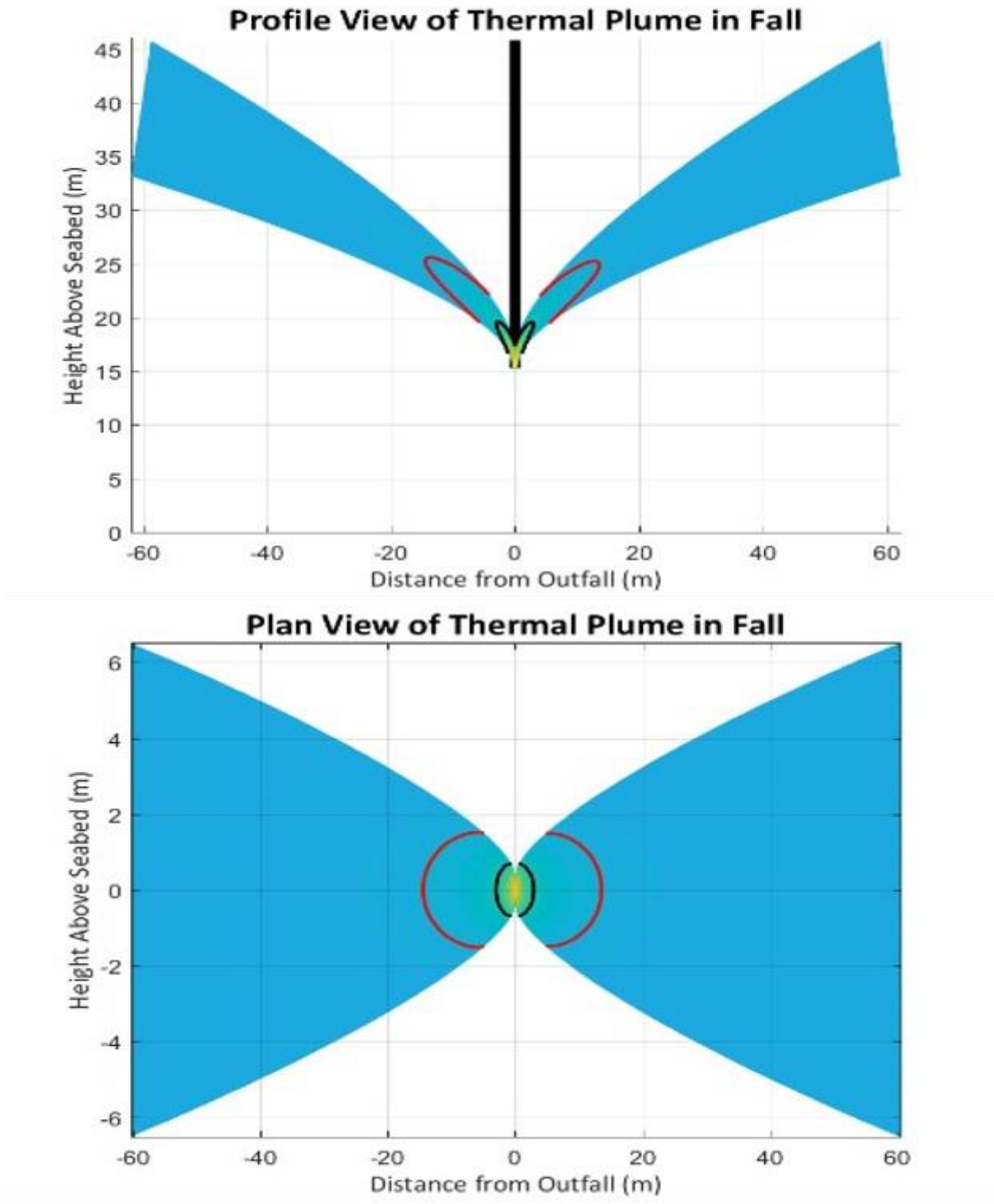

Figure 5-10. Profile view (top) and plan view (bottom) of the 30 m LMSL thermal plume in the NFR during winter.

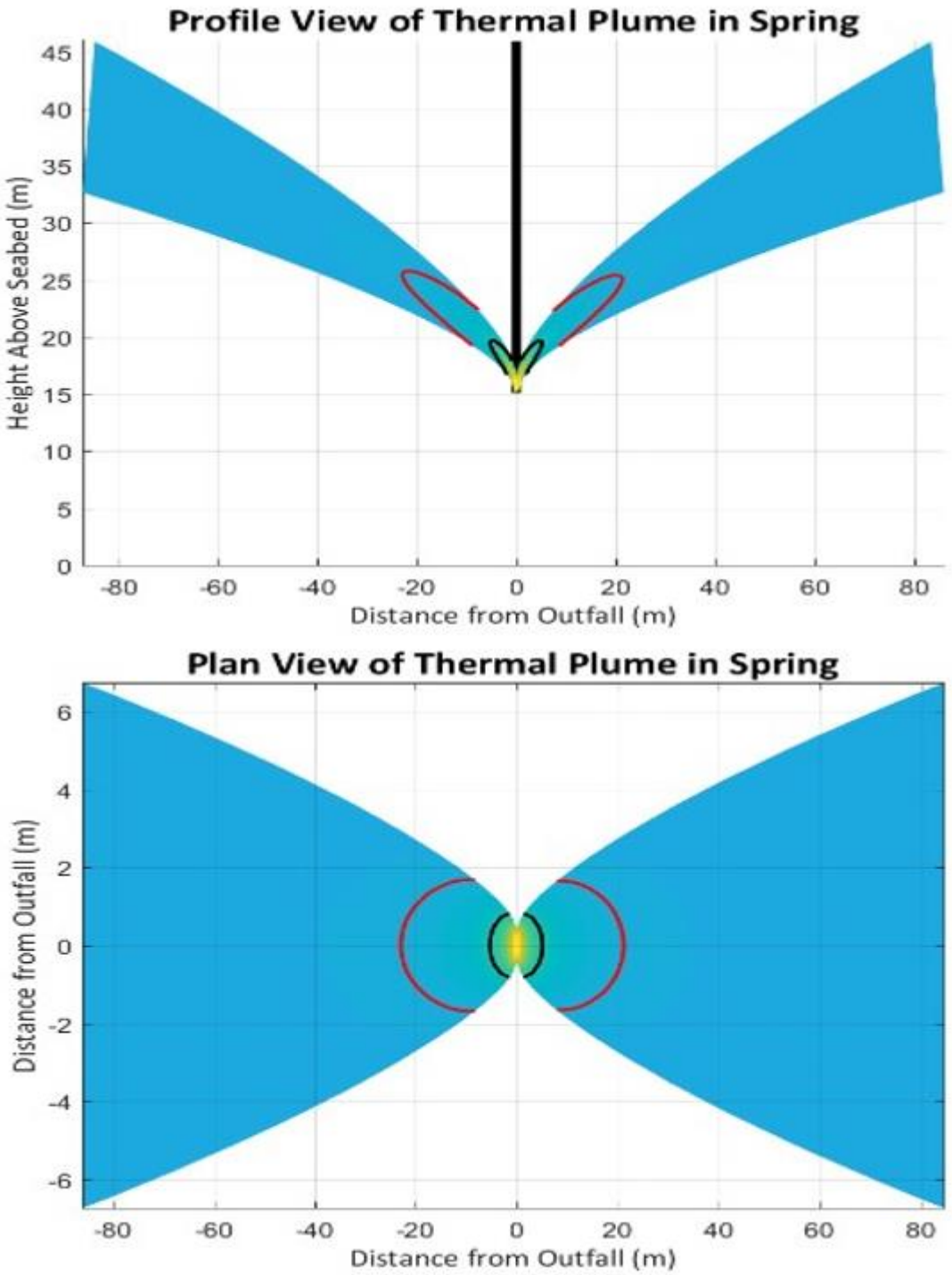

Figure 5-11. Profile view (top) and plan view (bottom) of the 30 m LMSL thermal plume in the NFR during spring.

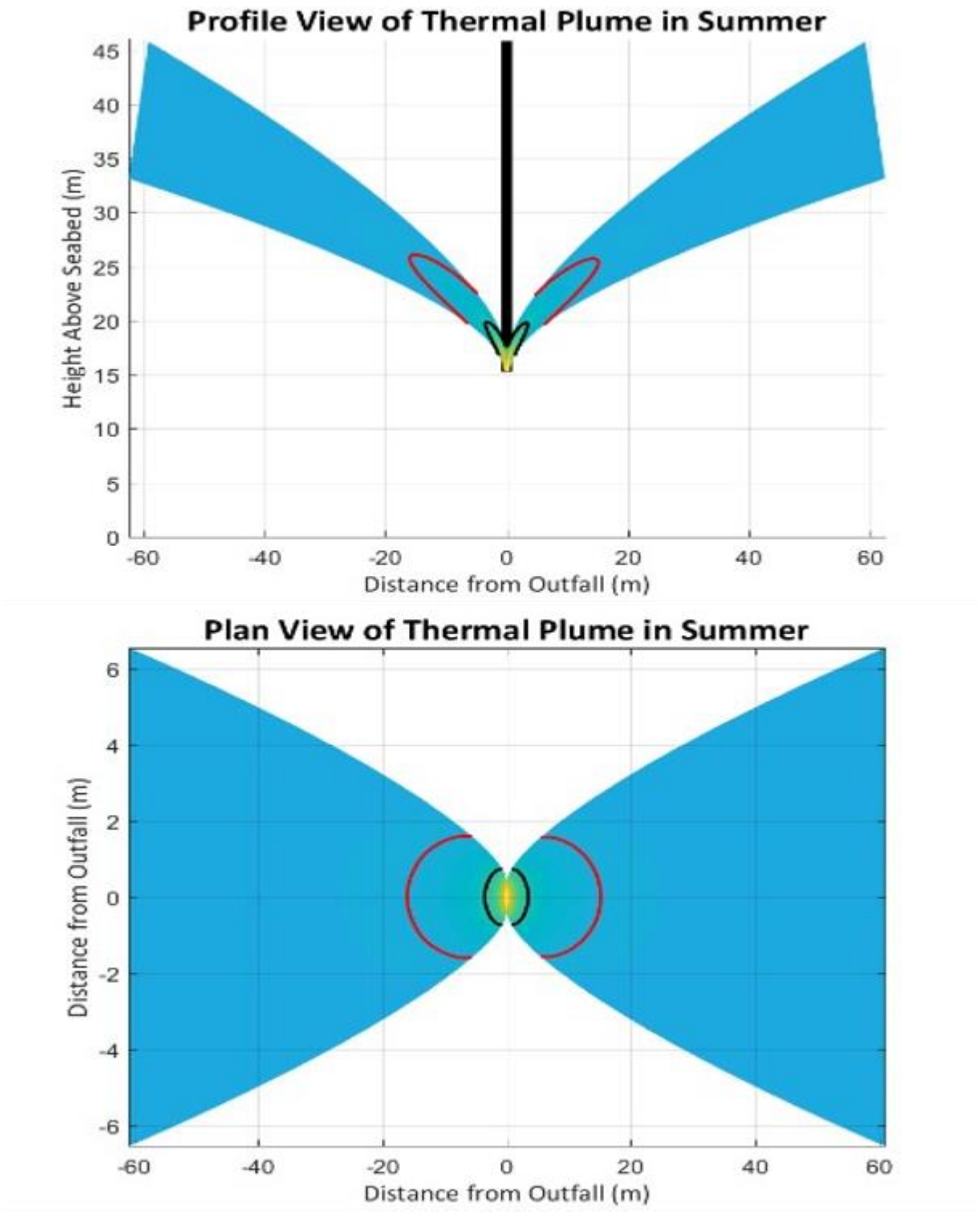

Figure 5-12. Profile view (top) and plan view (bottom) of the 30 m LMSL thermal plume after slack tide in the NFR during summer.

6.0 SUMMARY

Output from the NECOFS model was extracted from 45 vertical layers and used to inform the analyses of the OCS-DC intake HZI and thermal plume at the discharge. Stream function theory was used to develop a numerical solution to delineate the intake HZI which can be defined by velocity increases of 10% greater than ambient current velocities absent the intake. The 10% intake HZI threshold was simulated to extend below the intake pipe to a height of 19 ft (5.7 m) above the seabed (no seafloor intersection) in a 12 ft (3.7 m) radius around the CWIS for a total intake HZI of 463 ft^2 (43 m^2).

CORMIX model simulations were run for each season to assess the thermal plume associated with OCS-DC discharge and for three different discharge configurations. The winter and spring months were shown to have the largest temperature differentials, as defined by the extent of thermal plume above the 1°C ΔT (i.e., where temperature of discharged water is anticipated to be at least 1°C above ambient water temperature). The smallest plume size, defined by the 1°C change in temperature, for each configuration occurred for the fall simulations, while the largest plume occurred during spring simulations.

- The 18 ft (6 m) LMSL discharge depth and single discharge point had the largest plume area 3.1 hours after slack tide with and area of 602 ft^2 (55.9 m^2) and the smallest plume size of 419 ft^2 (38.9 m^2) before slack in the fall.
- The 40 ft (12 m) LMSL discharge depth and single discharge point had the largest plume area 3.1 hours after slack tide with and area of 731 ft^2 (66.9 m^2) and the smallest plume size of 415 ft^2 (38.6 m^2) after slack in the fall.
- The 100 ft (30 m) LMSL discharge depth and single discharge point had the largest plume area 3.1 hours after slack tide with and area of 613 ft^2 (56.9 m^2) and the smallest plume size of 316 ft^2 (29.3 m^2) before slack in the fall.

7.0 REFERENCES

Chow, V. T. (1959). *Open-Channel Hydraulics.* Caldwell, NJ: The Blackburn Press.

Doneker, R. L., & Jirka, G. H. (2007). *CORMIX User Manual.* Washington D.C.: U.S. Environmental Protection Agency.

Orsted. (2021). *SunRise Wind Construction & Operations Plan.* Fredericia, Denmark: Orsted & Eversource.

Trowbridge, J. (2021, July 1). Principal Investigator; Ocean Observatories Initiative. (A. K. (email correspondence), Interviewer)

UMass Dartmouth MEDM Lab. (2021, 7 12). *The Northeast Coastal Ocean Forecast System (NECOFS)*. Retrieved from Ubiversity of Massachussetts-Dartmouth School of Marine Science and Technology: http://fvcom.smast.umassd.edu/necofs/

Woods Hole Group. (2021). *Hydrodynamic and Sediment Transport Modeling Sunrise Wind Farm Project.* Bourne, MA: Woods Hole Group.

Young, D. F., Munson, B. R., Okiishi, T. K., & Huebsch, W. W. (2007). *A Brief Introduction to Fluid Mechanics.* New York: John Wiley and Sons.

Appendix A:

DESCRIPTION OF MODEL USED TO

ESTIMATE INTAKE HYDRAULIC ZONE OF INFLUENCE

To estimate the intake HZI associated with operation of the OCS-DC, Woods Hole Group employed an analytical model based on established stream function theory. This attachment describes the development of the model, which is based on standard governing equations of fluid dynamics, as well as the approach and assumptions applied to define the intake HZI. Due to the limited hydrodynamic data available, and anticipated modest scale of influence, this simple analytical model was selected as the appropriate approach to the estimate the intake HZI. The model determines the streamlines within the source water and includes background tidal velocities and the influence of water withdrawal activity. Two assumptions are made to determine the intake HZI. The first assumption is irrotational flow to simplify the solution of the differential equations. Although this assumption does not allow for the development of eddies within the fluid, it is assumed the scales of eddies are small in comparison to the scale of the HZI. The second assumption is constant depth (*h*) throughout the domain.

This attachment presents:

- the inputs necessary for solution of the governing equation,
- the governing equation, and
- the equations for this analytical model using the assumptions and governing equation.

A.1 INPUTS

Consider a semi-infinite body of water of constant depth *h*. Let *r* and *z* be cylindrical, planar coordinates, with *r = 0* corresponding to the center of the vertical intake pipe and *r > 0* corresponding to the source water. The intake is modeled as a line sink of uniform strength. The length of the intake is *L*, and the intake pipe is t between *r = -L/2* and *r = +L/2*. The total volumetric flowrate into the intake pipe is *Q*. The flow induced by the intake pipe is assumed to be irrotational. The velocity vector in the *r-z* coordinate system is (u_r, w). From continuity, the velocity at the intake pipe is $(u_r, w) = [0, -Q/(Lh)]$ at r *= 0.* The purpose of these notes is to determine the velocity $(u_r, w)$and the stream function ψ(r,z).

A.2 GOVERNING EQUATION AND MODEL DEVELOPMENT

The solution for the r component, u_r of the velocity proceeds by considering the contribution induced by a small segment of the intake pipe, and then summing these contributions over the entire length of the intake pipe. Consider a small segment of the intake pipe with position *(r,z) = (*r',0*)* and length *dr'*, which induces a velocity (du_r, dw) at an arbitrary position *(r,z)*. According to irrotational flow theory, the radial velocity du_{rr} induced at the position *(r,z)* by the segment of intake is

$$du_r = -\frac{Q}{Lz}\frac{dr'}{\pi R} \quad EQ.1$$

where $R = [z^2 + (r-r')^2]^{1/2}$ is the distance between *(r',0)* and *(r,z)*. It follows from elementary geometry that

$$dw = \frac{(z - z')}{R} du_r \quad EQ.2$$

so that

$$dw(r,z) = -\frac{1}{\pi}\frac{Q}{Lh}\frac{z - z'}{R^2}dz' = -\frac{1}{\pi}\frac{Q}{Lh}\frac{z - z'}{r^2 + (z - z')^z}dz' \quad EQ.3$$

The velocity *w(r,z)* is computed by integrating the contributions *dw* from all segments of the intake pipe; i.e.

$$w(r,z) = \int dw = -\frac{1}{\pi}\frac{Q}{Lh}\int_{-\frac{L}{2}}^{+\frac{L}{2}}\frac{z - z'}{r^2 + (z - z')^z}dz' = -\frac{1}{\pi}\frac{Q}{Lh}\int_{-\frac{L}{2}}^{+\frac{L}{2}}\frac{z' - z}{r^2 + (z' - z)^z}dz' \quad EQ.4$$

The integral can be evaluated in closed form, yielding

$$w(r,z) = \frac{1}{2\pi}\frac{Q}{Lh} ln\left[\frac{r^2 + (L/2 - z)^2}{r^2 + (L/2 + z)^2}\right] \quad EQ.5$$

From which *w(r,z)* can be calculated if desired.

By definition, the streamfunction ψ(r,z) is related to $u_r(r,z)$ by

$$\frac{\delta\Psi}{\delta z} = u_r \quad EQ.6$$

At the intake pipe ($r = 0$), u_r is given by

$$u_r(0,z) = 0 \; for \; z < -L/2 \quad EQ.7A$$

$$u_r(0,z) = \frac{-Q}{Lh} \; for \; -L/2 < z < +L/2 \quad EQ.7B$$

$$u_r(0,z) = 0 \; for + L/2 < Z \quad EQ.7C$$

It follows from (EQ. 6) and (EQ. 7) that at the intake pipe ψ is given by

$$\psi(o,z) = +\frac{Q}{2h} \; for \; z \leq L/2 \quad EQ.8A$$

$$\psi(o,z) = -\frac{Q}{2h} \; for - {}^{L}/_{2} < z < {}^{L}/_{2} \quad EQ.8B$$

$$\psi(o,z) = -\frac{Q}{2h} \; for + {}^{L}/_{2} < z \quad EQ.8C$$

By definition, the stream function ψ is related to *w(r,z)* by

$$\frac{\delta\psi}{\delta r} = -w \;\; EQ.9$$

It follows from integration of (9) with respect to *x* that ψ is given by

$$\psi(r,z) = \varphi(o,z) - \int_0^r w(r',z)dr' \;\; EQ.10$$

where *r'* is a dummy variable of integration. The stream function can now be computed from (EQ. 5), (EQ. 8) and (EQ. 10). Numerical evaluation of the integral in (EQ. 10) is required.

As noted previously, the velocity *w(r,z)* is given explicitly by (EQ. 5). If desired, the velocity $u_r(r,z)$ can be calculated numerically from (EQ. 6) by means of finite differences once ψ(r,z) has been determined.